

A REPRODUCEABLE NOISE GENERATOR

by

DONALD GEORGE WATTS

B.A.Sc., University of British Columbia, 1956

A THESIS SUBMITTED IN PARTIAL FULFILMENT OF
THE REQUIREMENTS FOR THE DEGREE OF
MASTER OF APPLIED SCIENCE

in the Department

of

Electrical Engineering

We accept this thesis as conforming to the
standards required from candidates for the
degree of Master of Applied Science

Members of the Department
of Electrical Engineering

The University of British Columbia

April, 1958

Abstract

This thesis describes the design of a device for generating a reproduceable noise signal. The noise signal is generated by adding three periodic waveforms having non-multiple periods. Pulse techniques are used in the generation of the member functions so that the output may be reproduced exactly.

Theoretical and experimental determinations of the amplitude probability distribution and of the autocorrelation function of the signal were made. On the basis of tests and observations made, it is concluded that the signal generated may be considered a noise signal having a near-Gaussian amplitude probability distribution, very little correlation for time-shifts greater than 30 seconds, and a bandwidth of about 60 cps.

In presenting this thesis in partial fulfilment of the requirements for an advanced degree at the University of British Columbia, I agree that the Library shall make it freely available for reference and study. I further agree that permission for extensive copying of this thesis for scholarly purposes may be granted by the Head of my Department or by his representative. It is understood that copying or publication of this thesis for financial gain shall not be allowed without my written permission.

Department of Electrical Engineering,

The University of British Columbia,
Vancouver 8, Canada.

Date April 15, 1958

Acknowledgment.

The author is indebted to the Defence Research Board, Department of National Defence, Canada, for sponsoring the research project under Grant Number DRB C-9931-02 (550-GC).

Acknowledgment is gratefully given Dr. E. V. Bohn, under whose guidance this work was performed, and to Dr. F. Noakes, grantee of the project. Thanks, too, are extended to the U.B.C. Computing Centre for computer time and to the Van de Graaff Section of the U.B.C. Physics Department for granting time on the kicksorters. The author would like to thank Mr. R. M. Pye for writing the programme for the autocorrelation determination, and would also like to express his appreciation for the helpful suggestions received from other members and Graduate Students of the Electrical Engineering Department.

The author is indebted to the National Research Council of Canada for the assistance received through a post-graduate bursary granted in 1956 and to the Defence Research Board of Canada for assistance received while on a Research Assistantship.

Table of Contents

Abstract		page ii
Acknowledgment		vi
1. Introduction		1
2. Generation of a Noise Signal Using Periodic Functions		5
2-1. Introduction		5
2-2. Theory of Generation of the Noise Signal		5
2-2-1. The Period of a Composite Function		6
2-2-2. The Near-period of a Composite Function		7
2-3. Designing the Noise Generator		8
2-3-1. Generation of a Member Function		9
2-3-2. Determination of the Periods of the Member Functions		12
2-3-3. Summing of the Member Functions		14
3. Practical Design Considerations		15
3-1. Introduction		15
3-2. Electronic Circuitry		15
3-3. Scaling and Addition of Component Waveforms		15
4. Analysis of the Noise Signal		18
4-1. Introduction		18
4-2. Theoretical Analysis		18
4-2-1. Theoretical Amplitude Probability Distribution		18
4-2-2. Theoretical Autocorrelation Function		20
4-3. Experimental Analysis		24
4-3-1. Experimental Amplitude Probability Distribution		24
4-3-2. Experimental Autocorrelation Function		26
4-4. Comparison of Theoretical and Experimental Results		28
5. Conclusions		31
APPENDIX A.		
A-1. Programme for Determining the Near-period of a Function		33
A-2. Computer Results		34

APPENDIX B.

B-1. Programme for Determining the Theoretical Probability Distribution of Amplitudes	36
B-2. Computer Results	39

APPENDIX C.

C-1. Programme for Determining the Cardinal Points of the Theoretical Autocorrelation Function	43
C-2. Computer Results	44

APPENDIX D. References	46
----------------------------------	----

List of Illustrations

Figure		page
1-1.	Quasi-linearization of a Servomechanism	3
1-2.	Correlation of Signals	4
2-1.	Example Output Waveform from Multivibrator Chain	11
3-1.	Block Diagram of Noise Generator to follow	15
3-2.	100Kc Pulse Generator to follow	15
3-3.	Phantastron Divider Circuit to follow	15
3-4.	Multivibrator and Gating Circuits to follow	15
3-5.	Output Network	16
4-1.	Amplitude Probability Distributions to follow	18
4-2.	Theoretical Normalized Amplitude Probability Distribution to follow	19
4-3.	Sample Function	21
4-4.	Theoretical Normalized Autocorrelation Functions to follow	23
4-5.	Sampling System Schematic to follow	25
4-6.	Chopper and Differentiator Circuit to follow	25
4-7.	Experimental Normalized Amplitude Probability Distribution to follow	26
4-8.	Experimental Normalized Autocorrelation Function	27
4-9.	Block Diagram of Correlator	28
4-10.	Integrator Circuit Diagram to follow	28
4-11.	Normalized Probability Distributions to follow	28
4-12.	Alternate Form of Dissociation of Noise Signal	29
4-13.	Theoretical and Experimental Autocorrelation Functions	30
B-1.	Theoretical Normalized Amplitude Probability Distributions for two Member Function Sets to follow	41
C-1.	Theoretical Normalized Autocorrelation Functions to follow	44

A REPRODUCEABLE NOISE GENERATOR.

1. Introduction.

Noise generators are finding extensive applications in analogue computer systems^{7,19} and in servomechanism analysis.^{5,13,22}

In most applications, the signal is derived from conventional noise sources^{2,3,23,} for instance, the fluctuating component of the plate voltage of a thyratron kept in a condition of constant discharge, or the fluctuating component of the current in a conducting diode. The most important characteristic of these signals and of any noise signal is that the signal is random - that is, it should be impossible for all τ to specify the value of the function at a time $T + \tau$, knowing completely the behaviour of the function from time 0 to T . The noise signal is usually described in terms of its probability distribution functions. The most important of these are the first probability function which determines the distribution of signal amplitudes and the second probability distribution which determines the autocorrelation function of the signal. In physical systems subject to statistical fluctuations, the first probability distribution of the fluctuations is usually Gaussian and the autocorrelation function $\phi(\tau)$ decreases rapidly to 0 as τ increases.

In digital computers random numbers can be generated by various methods^{10,11} and this would be the equivalent of the noise generator in an analogue computer²⁴. Since the digital computer has only a finite number of states the sequence of random numbers

must have a finite period and therefore cannot be truly random. This pseudo-random sequence is reproduceable since it is generated by a pre-determined programme. This reproduceability has certain attractive features associated with it which the physical noise generator does not possess. For certain analogue computer studies it would be desirable to have a reproduceable pseudo-noise signal similar to the pseudo-random number sequence generated by a digital computer.

This thesis is concerned with the design and development of an electronic device for generating a reproduceable noise signal. The applications of this noise generator and conventional noise generators in servomechanism design are discussed in the following paragraphs.

The design of a control system depends upon the nature of the input functions, random disturbances, (such as uncontrolled load disturbance or noise in amplifiers) and the nature of the desired response.^{5,13,15,22} Usually these functions can only be described statistically, and hence the mechanism is designed according to statistical design theory.^{4,5,13,15,22} This requires a determination of the average characteristics of the signal, the choice of the measure of the error, and the design of the system in accordance with the conditions of error minimization. Unfortunately, a general mathematical analysis of control systems seems limited to linear systems,⁵ and to minimization of the mean-square error. Thus, if another criterion for minimum error is chosen, or if a nonlinear system is analyzed, the recourse is to experimental methods.^{5,14}

As an example, consider the quasi-linearization of a nonlinear servomechanism. The nonlinear element is approximated by a quasi-linear element.⁵ The linearized system is then designed so that the response of the linear system to an input $\phi_{ii}(\tau)$ is $\phi_{io}(\tau)$ where $\phi_{ii}(\tau) = \overline{y_i(t) y_i(t+\tau)}$, $\phi_{io}(\tau) = \overline{y_i(t) y_o(t+\tau)}$, and $y_o(t)$ is the output of the nonlinear system to an input $y_i(t)$. The process is shown diagrammatically in Figure 1-1.

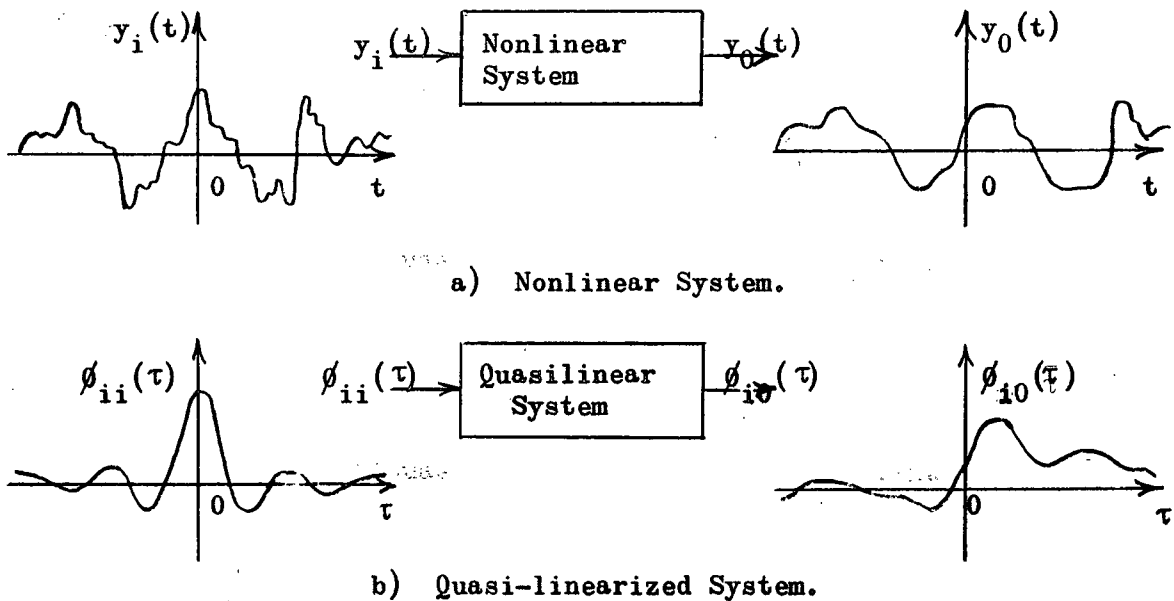


Figure 1-1. Quasi-linearization of a Servomechanism.

The equivalent system can then be analyzed for behaviour with respect to changes in system parameters or changes in input signal characteristics, and hence a better understanding of the nonlinear system may result. In order to design the equivalent linear system, the input autocorrelation function $\phi_{ii}(\tau)$ and the input-output cross-correlation

function $\phi_{i0}(\tau)$ must be determined. With a conventional noise generator as the signal source, complex autocorrelators^{1,21,22} or variable delay lines would have to be used in order to be able to calculate the functions $\phi_{ii}(\tau)$ and $\phi_{i0}(\tau)$. With two of the reproduceable noise generators, however, only simple multiplying and averaging devices would be needed to determine these functions, since $y_i(t)$ and $y_i(t+\tau)$ could be generated simply by turning one of the generators on a time τ before the other one. (See Figure 1-2)

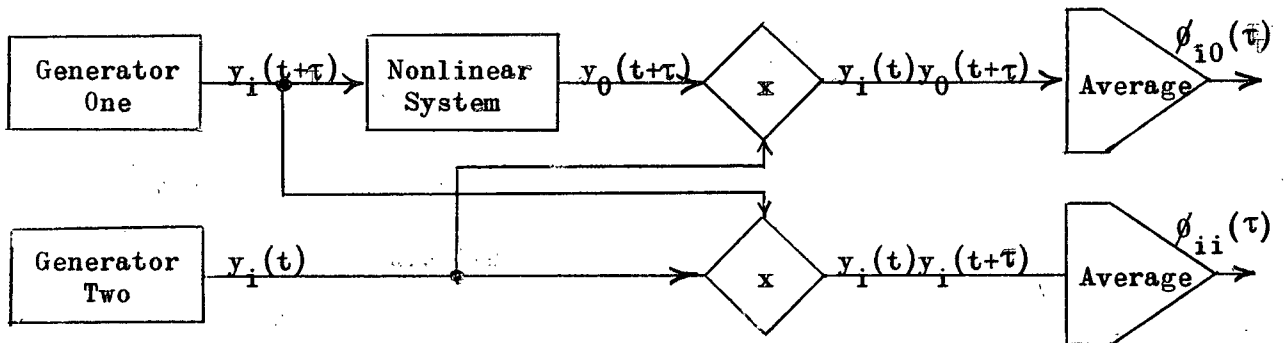


Figure 1-2. Correlation of Signals.

Also, if the input signal were obtained from a conventional noise generator, the effect of varying a parameter in the linear system would have to be evaluated statistically whereas if a reproduceable noise generator were used a fast comparison of the responses of the altered and unaltered system to the same random signal would be possible. Thus the design of both linear and nonlinear servomechanisms subject to minimization of various error criteria could be facilitated using the reproduceable noise generator.

2. Generation of a Noise Signal Using Periodic Functions

2-1. Introduction.

Since a noise signal is specified only by its probability distribution functions,^{3,23} there is no definite approach to the problem of generating a reproduceable noise signal. For the probable applications of this generator it is more important to have the signal amplitude fluctuate according to a definite probability distribution than it is to have an autocorrelation function which falls off rapidly with increasing τ . The signal output will therefore be required to have a first probability distribution which is approximately Gaussian, and an autocorrelation function which falls off as rapidly as possible with increasing τ , due consideration being given to achieving this result with simple circuitry.

2-2. Theory of Generation of the Noise Signal.

To meet these requirements it was proposed that the signal be generated as the sum of a number of periodic functions, under the assumption that the signal so produced would fluctuate in a haphazard manner. Because periodic member functions are used, the composite function is also periodic. If the noise signal is to be random in a time interval, however, the signal must not repeat in that interval; hence, the composite function must have a long period. There is also a time of recurrence or near-period associated with a composite function of this form which may be very much shorter than the period of the function. Consequently, a further restriction is made on the function; that is, the near-period should be as long as possible.

2-2-1. The Period of a Composite Function.

A function $F(t)$ composed of a number of periodic functions $f_i(t)$ ($i = 1, 2, \dots, m$), such that $F(t) = \sum_{i=1}^m f_i(t)$, has a period which is dependent upon the periods of the component functions. To determine the relationship between the period of $F(t)$ and the periods of $f_i(t)$ consider the function

$$F(t) = \sum_{i=1}^m f_i(t) = f_1(t) + f_2(t) + \dots + f_m(t)$$

where $F(t) = F(t + \tau)$,

and $f_i(t) = f_i(t + \tau_i)$.

That is, τ is the period of $F(t)$ and τ_i is the period of $f_i(t)$.

Then $F(t) = f_1(t) + f_2(t) + \dots + f_m(t) = F(t + \tau)$

and so $F(t + \tau) = f_1(t + \tau) + f_2(t + \tau) + \dots + f_m(t + \tau)$

Since $f_i(t) = f_i(t + \tau_i) = f_i(t + n \tau_i)$ where n is an integer, then

we must have $n_1 \tau_1 = n_2 \tau_2 = \dots = n_m \tau_m = \tau$.

(n_1, n_2, \dots, n_m integers)

If we let the largest common divisor^{*} of $\tau_1, \tau_2, \dots, \tau_m$ be T , then we may write $\tau_1 = \lambda_1 T$, $\tau_2 = \lambda_2 T$, \dots , $\tau_m = \lambda_m T$, where $\lambda_1, \lambda_2, \dots, \lambda_m$ are dimensionless integral multipliers whose largest common divisor is 1.

That is, T defines a unit period and the periods of the functions are multiples of this unit period. Then, writing $\tau = \lambda T = n_1 \lambda_1 T = n_2 \lambda_2 T = \dots = n_m \lambda_m T$ we have $\lambda = n_1 \lambda_1 = n_2 \lambda_2 = \dots = n_m \lambda_m$. In the general case λ

* The largest common divisor of the numbers a, b, c, \dots, k , is the largest positive integer which divides a, b, c, \dots, k .¹²

equals the least common multiple* of $\lambda_1, \lambda_2, \dots, \lambda_m$. In the special case where $\lambda_1, \lambda_2, \dots, \lambda_m$ are all coprime**, the least common multiple of $\lambda_1, \lambda_2, \dots, \lambda_m$ is simply the product $\lambda_1 \cdot \lambda_2 \cdot \dots \cdot \lambda_m$. The period in this case is $\tau = \lambda T = \lambda_1 \cdot \lambda_2 \cdot \dots \cdot \lambda_m T$. Thus it is seen that if the periods of the member functions are chosen so that the λ_i 's are coprime, the composite function will have a very long period.

2-2-2. The Near-period of a Composite Function.

A function obtained by summing two or more periodic functions may exhibit what shall be termed near-periodicity. To illustrate the phenomena of near-periodicity and to establish a criterion for determining the near-period of a function, consider the function

$$F(t) = f_1(t) + f_2(t),$$

where

$$f_1(t) = f_1(t + \lambda_1 T),$$

$$f_2(t) = f_2(t + \lambda_2 T),$$

and λ_1, λ_2 , and T are as defined in the preceding section.

The multipliers λ_1 and λ_2 are necessarily coprime and the period of $F(t)$ is $\lambda T = \lambda_1 \lambda_2 T$. Suppose, however, that there are integers $n_1 (< \lambda_2)$ and $n_2 (< \lambda_1)$ such that $n_1 \lambda_1 \approx n_2 \lambda_2$.

* The least common multiple of the numbers a, b, c, \dots, k is the least positive number which is divisible by a, b, c, \dots, k .¹²

** Two integers a and b are said to be coprime if the largest integer which divides both a and b is 1. The numbers a, b, c, \dots, k , are said to be coprime if every two of them are coprime.¹²

That is $n_1 \lambda_1 = n_2 \lambda_2 + \delta_2$ $(|\delta_2| \ll \lambda_1 \text{ or } \lambda_2)$
 $(\delta_2 \geq 0)$

Then,

$$\begin{aligned} F(t + n_1 \lambda_1 T) &= f_1(t + n_1 \lambda_1 T) + f_2(t + n_1 \lambda_1 T) = \\ &= f_1(t + n_1 \lambda_1 T) + f_2(t + n_2 \lambda_2 T + \delta_2 T) = \\ &\approx f_1(t + n_1 \lambda_1 T) + f_2(t + n_2 \lambda_2 T) = \text{(neglecting } \delta_2 T \text{ w.r.t. } \lambda_2 T) \\ &= f_1(t) + f_2(t). \end{aligned}$$

or, $F(t + n_1 \lambda_1 T) \approx F(t)$.

We see that the function almost repeats in the time $n_1 \lambda_1 T$.

We shall call this time (T_n) , the near-period of the function $F(t)$. Of course, the value of T_n is dependent upon δ , the maximum allowed value of δ_2 . If the value of δ is chosen to be 0, then T_n is simply the period of the function, $\lambda_1 \lambda_2 T = \lambda T$.

In the general case where $F(t) = \sum_{i=1}^m f_i(t)$ and

$$f_i(t) = f_i(t + \lambda_i T)$$

we shall define the near-period T_n of $F(t)$ to be the value $n_1 \lambda_1 T$.

The n_i ($i = 1, 2, \dots, m$) are integers which satisfy the conditions

$$|\delta_{ij}| \ll \delta \quad \text{where} \quad \delta_{ij} = (n_i \lambda_i - n_j \lambda_j)$$

$$i, j = 1, 2, \dots, m$$

and where δ is small compared to $\lambda_1, \lambda_2, \dots, \lambda_m$.

2-3. Designing the Noise Generator.

The design of the noise generator consisted of a choice of the form of the member functions and the determination of the number and periods of the member functions so as to produce a long near-period.

The form of the member functions was first decided upon from considerations of ease and reliability of generation with electronic circuitry. Because reproduceability was a prime consideration, a combination of pulse and digital techniques was used. Once the form of the member functions had been adopted, computations were made to determine the number and the periods of these functions so as to yield a long near-period of the composite function. The form of the member functions is best described by considering the manner in which the member functions are generated and the results of this method of generation.

2-3-1. Generation of a Member Function.

Each member function is generated as the result of the continuous cycling of a multivibrator chain by a precision-timed pulse train. A 100 Kc crystal oscillator serves as the source from which are derived the actuating pulses for the multivibrator chains.

Consider the generation of one of these member functions. The output of the crystal oscillator is used to initiate a continuous pulse output with a pulse-recurrence-frequency (PRF) of 100,000 pulses per second (pps). This output PRF is divided down successively by three phantastron divider units whose division ratios - that is the ratios of the input PRF's to the output PRF's - are d_1 , d_2 , and d_3 . The PRF of the output of the last phantastron is then $\frac{100,000}{d_1 d_2 d_3}$ pps. This output is used to actuate a multivibrator chain consisting of k bistable multivibrators in series. The multivibrator chain is designed so that one cycle of the chain is equivalent to N pulses, where $N = (2^k - 1)$. The period of the chain is then $\frac{N d_1 d_2 d_3}{100,000}$ seconds.

Each multivibrator of the chain actuates a gate so that a voltage V_j ($j = 1, 2, \dots, k$) is transmitted to the output of the generator when the multivibrator is in one state and a voltage 0 when the multivibrator is in the other state. The voltages V_j are either positive or negative. The output voltage at any instant is the sum of the voltages transmitted to the output of the generator.

To illustrate the waveform obtained at the output of the generator from one of the multivibrator chains, consider the output of a chain consisting of three multivibrators connected so that

$V_1 = +3V$, $V_2 = -2V$, and $V_3 = -V$, and the chain is connected so that it recycles after $(2^3 - 1) = 7$ pulses. The initial configuration is

such that the output voltage V_o is 0. After one pulse, $V_o = V_1 = \dots +3V$

two pulses, $V_o = V_1 + V_2 + V_3 = \dots +0V$

three pulses, $V_o = V_3 = \dots -1V$

four pulses, $V_o = V_1 + V_3 = \dots +2V$

five pulses, $V_o = V_2 = \dots -2V$

six pulses, $V_o = V_1 + V_2 = \dots +1V$

seven pulses, $V_o = 0 + 0 + 0 = \dots -0V$

The cycle repeats after the seventh pulse. The sequence of operation depends entirely upon the initial configuration of the multivibrators.

The output waveform is shown in Figure 2-1.

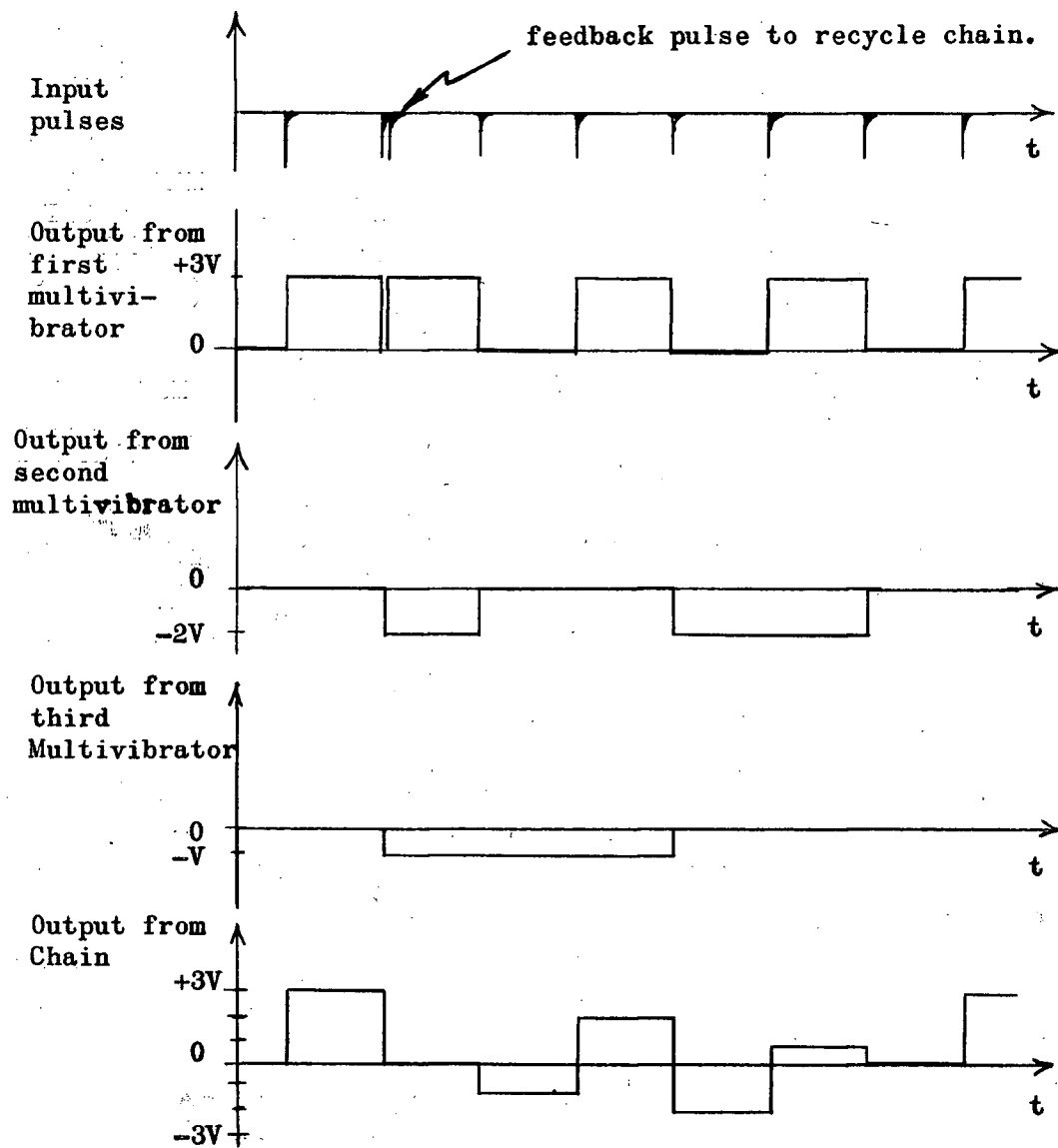


Figure 2-1. Example Output Waveform from Multivibrator Chain.

The waveform described above illustrates the form of the member function adopted for use in the noise generator. The remaining step in the design was to obtain a long near-period for the composite function.

2-3-2. Determination of the Periods of the Member Functions.

The final step in the design was to determine the number of member functions and the periods of the member functions so as to obtain a long near-period of the output signal. (At this point, no idea of what constituted a "long" near-period had been formulated.) The simplest form of the composite function was tried, namely $F(t) = f_1(t) + f_2(t)$ where the member functions were of the form described in the preceding section.

The period of $f_1(t)$ is $\tau_1 = \frac{N_1 d_{11} d_{12} d_{13}}{100,000}$ secs, and that of $f_2(t)$ is $\tau_2 = \frac{N_2 d_{21} d_{22} d_{23}}{100,000}$ secs. The problem was to determine values of the N 's and d 's which would give a long near-period. Because phantatron dividers were to be used, the d 's were constrained to lie in the range 7 to 20 to ensure stable operation. Also, the product $d_1 d_2 d_3$ was to be about 1000 so that the input PRF to the multivibrator chains would be about 100 pps. The N 's were chosen to be of the form $(2^k - 1)$ so the factors N_1 and N_2 would be coprime. The k 's were kept small so as to minimize the biasing effect inherent in the binary scaling action of the multivibrator chains. (viz. the last multivibrator in a chain is "off" for $(\frac{2^k}{2} - 1)$ successive pulses and "on" for $\frac{2^k}{2}$ successive pulses: this merely produces a shift in the output dc level every half cycle, and hence if the k 's are too large this may be considered a sort of "biasing" action as opposed to the "switching" action of the first multivibrators.)

In order to determine values of the d 's and k 's for the two-function case, a programme was written for the Alvac III E computer to solve the problem: Given δ , K and M Compute integers x and z so that

the difference $\delta_1 = (xK - zM)$ in absolute value is less than or equal to δ .

(i.e. $|\delta_1| \leq \delta$) Various values of $K = (2^{k_1} - 1)d_{11}d_{12}d_{13}$ and

$M = (2^{k_2} - 1)d_{21}d_{22}d_{23}$ were tried, but the length of the near-periods obtained (as determined for $\delta = \frac{d_{11}d_{12}d_{13}}{20}$) were all only of the order of a few seconds. This was considered too short.

The next simplest form of the composite functions was tried, that of $F(t)$ equal to the sum of three member functions. Again, a programme was written for the Alvac III E computer to solve the problem:

Given δ , K , L , and M Compute integers x , y , and z , so that the differences

$\delta_1 = (xK - zM)$ and $\delta_2 = (yL - zM)$ are, in absolute value, less than

or equal to δ . Various values of $K = (2^{k_1} - 1)d_{11}d_{12}d_{13}$,

$L = (2^{k_2} - 1)d_{21}d_{22}d_{23}$ and $M = (2^{k_3} - 1)d_{31}d_{32}d_{33}$ were tried. Near periods

ranging from a few seconds to six minutes were obtained. The values

which gave a near-period of six minutes are the values used in the

noise generator.

They are:

d_{11}	= 10	d_{21}	= 10	d_{31}	= 10
d_{12}	= 13	d_{22}	= 11	d_{32}	= 12
d_{13}	= 8	d_{23}	= 9	d_{33}	= 8
$(2^{k_1} - 1)$	= 7	$(2^{k_2} - 1)$	= 15	$(2^{k_3} - 1)$	= 31

In this case, the values of the λ 's are

$$\begin{aligned}\lambda_1 &= 728 = 7(13)8 \\ \lambda_2 &= 1485 = 15(11)9 \\ \lambda_3 &= 2976 = 31(12)8\end{aligned}$$

and that of T , $T = \frac{10}{100,000}$ seconds = 0.1 milliseconds.

The period of the function, given by T times the least common multiple

of λ_1 , λ_2 and λ_3 is:

$$\tau = \frac{728(1485)2976(0.1)}{3(8)} \text{ milliseconds} = 13,405,392.0 \text{ msec.},$$

which is approximately 223 minutes. The near-period, T_n , as determined for $\delta = \frac{d_{11}d_{12}d_{13}}{20}$ is:

$$T_n = n_1 \lambda_1 T = 5069(728)(0.1) \text{ msec} = 369,023.2 \text{ msec.},$$

which is approximately six minutes. (The value of δ chosen is such that δT is about one-half the time between pulses into the chains.) The programme for the three-function case is described in Appendix A.

2-3-3. Summing of the Member Functions.

Addition of the three member functions is effected through an operational amplifier circuit using a Philbrick K2-X operational amplifier unit²⁰. The member functions are summed and passed through a smoothing network simultaneously and in this way the output is smoothed into a continuous signal.

3. Practical Design Considerations

3-1. Introduction.

This section presents the circuits used in the noise generator and a discussion of the manner in which the member function waveform voltages and the output network parameters were decided upon.

3-2. Electronic Circuitry.

All the circuits used in the noise generator are of standard design. For this reason, no descriptions of the circuit actions are given and instead the reader is referred to standard texts and journals. (References 6, 17, 18, and 19.) A block diagram of the noise generator and diagrams of the circuits used in the noise generator are given in Figures 3-1 to 3-4 inclusive. Component values are included in the circuit diagrams as well as some of the pertinent waveforms.

3-3. Scaling and Addition of Component Waveforms.

The form of the member functions having been decided, the next step was to choose values of the output waveform voltages. In order to further minimize the biasing effects of the binary scaling action of the multivibrator chains (Section 2-3-2.) it was decided to weight the output voltages gated by the multivibrators. For example, for a chain of k multivibrators, the weighting factors are such that $V_1 = \frac{1}{1} V$, $V_2 = \frac{1}{2} V$, \dots , $V_k = \frac{1}{k} V$. Also, the voltages were chosen so that the sum of the positive voltages gated by the chain was equal to the sum of the negative voltages gated by the chain. (i.e.,

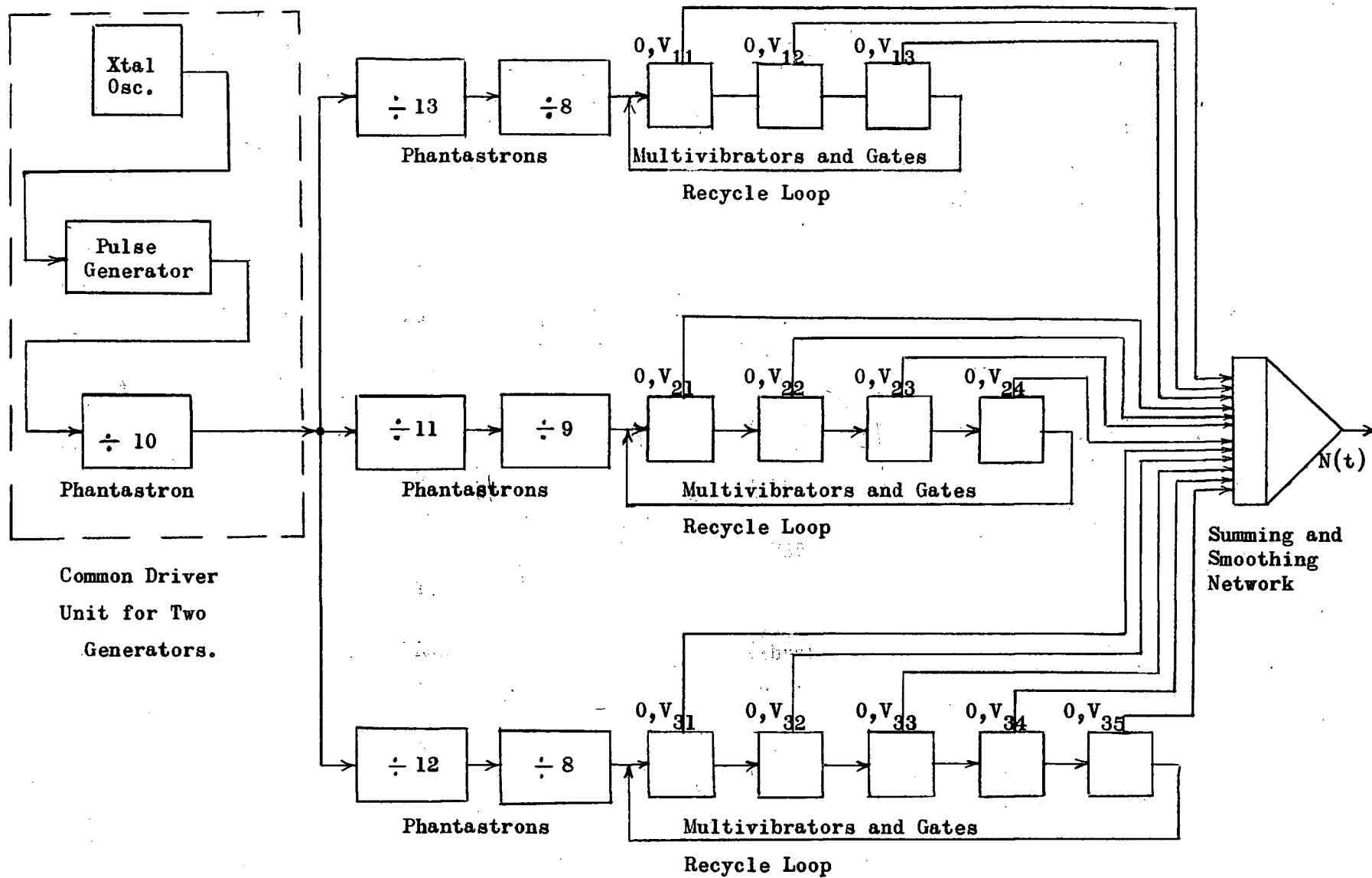
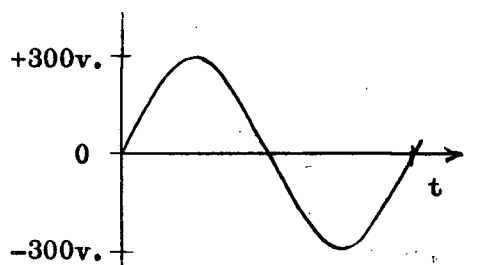
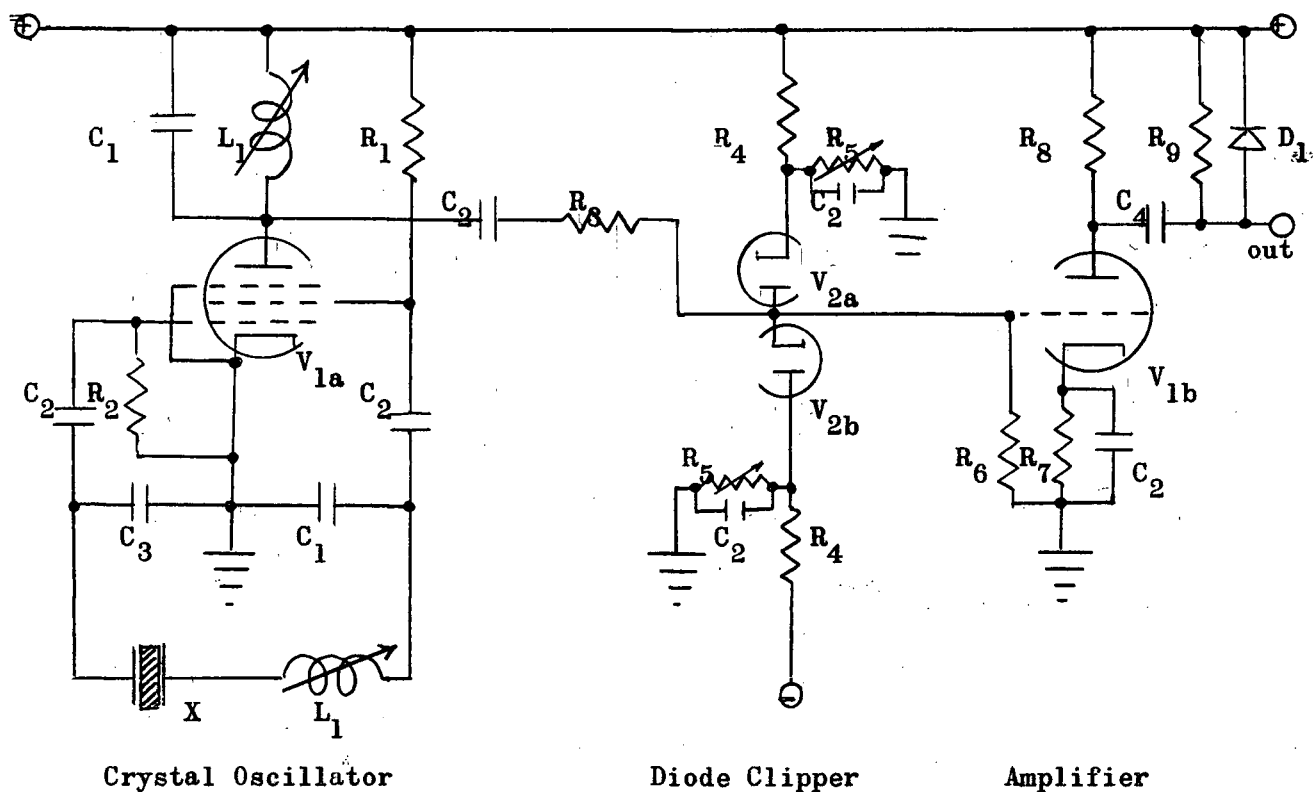
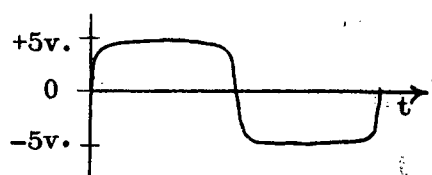


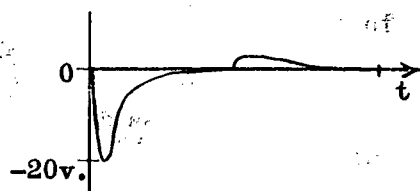
Figure 3-1. Block Diagram of Noise Generator.



Output of Crystal Oscillator



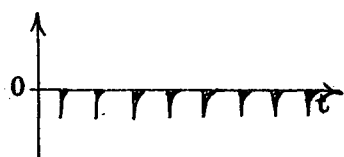
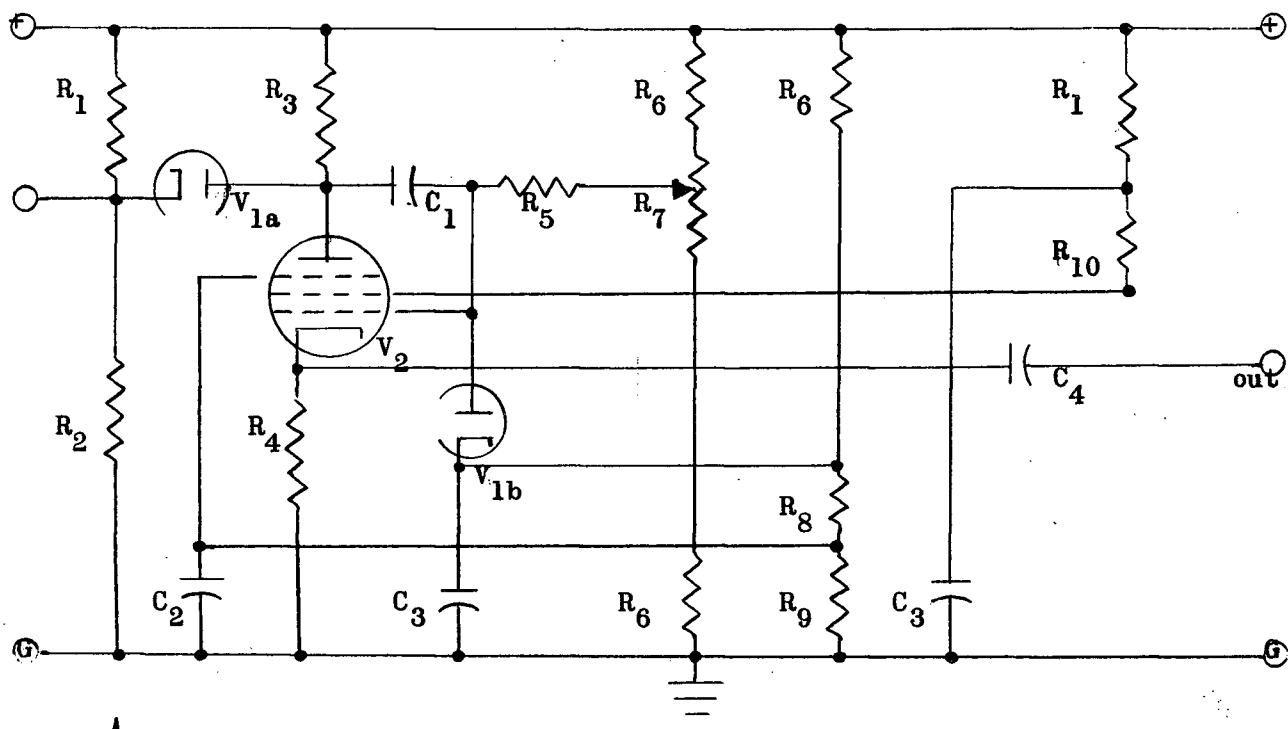
Output of Diode Clipper



Differentiated Output of Amplifier

R ₁150K	1 watt
R ₂1MEG	1/2 "
R ₃ 39K	" "
R ₄270K	" "
R ₅ 5K	" " pot.
R ₆470K	" "
R ₇470K	" "
R ₈ 15K	2 " "
R ₉ 22K	1/2 "
C ₁250pf	
C ₂	...0.01μf	
C ₃	...4000pf	+ = +300 volts
C ₄ 25pf	- = -300 volts
L ₁ 10mh	
X ₁ 100Kc crystal	
V ₁	...6AN8	
V ₂	...6AL5	
D ₁	...1N191	

Figure 3-2. 100Kc Pulse Generator.



Input Pulses

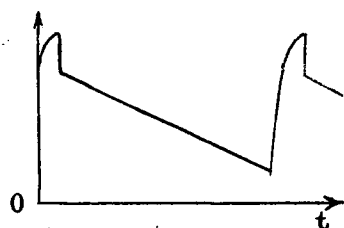
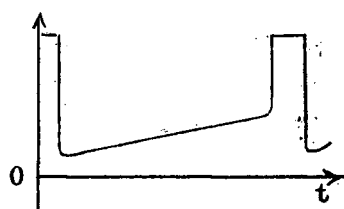
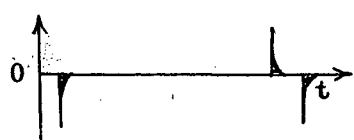


Plate Waveform



Cathode Waveform



Differentiated Cathode Waveform

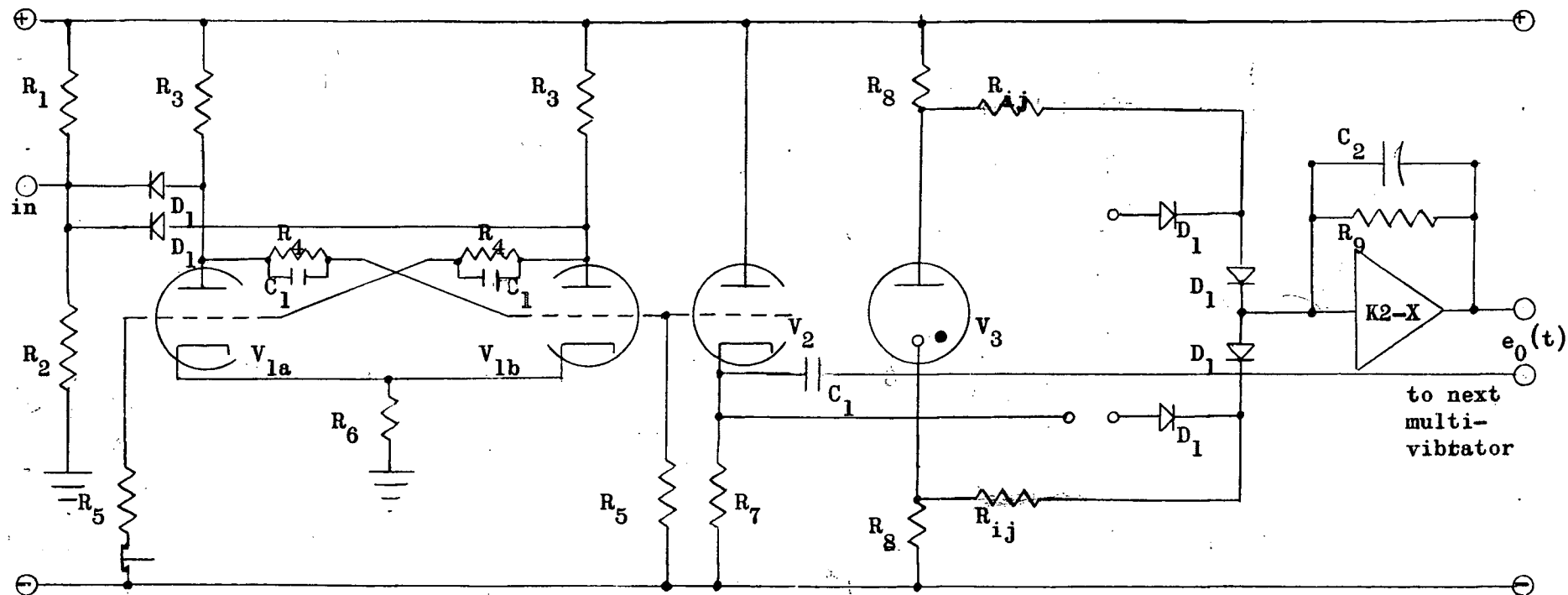
R ₁ 22K
R ₂220K
R ₃6.8K
R ₄100K
R ₅200K
R ₆ 10K
R ₇ 9K
R ₈4.7K
R ₉0.05μf
R ₁₀0.25μf
C ₁250 pf
C ₂6AL5
C ₃6AS6
C ₄	

+ = +300 volts

- = -300 volts

Input PRF (pps)	100,000	10,000	1,000
Division Ratio	10	11,12,13	8,9
R ₃	39K	68K	100K
R ₅	9.4MEG	9.4MEG	10MEG
C ₁	50pf	250pf	1000pf

Figure 3-3. Phantatron Divider Circuit.



Bistable Multivibrator

Cathode Follower

Gating Circuits

Output Stage

R_1 270K $\frac{1}{2}$ watt
 R_2 470K " "
 R_3 100K " "
 R_4 150K " "
 R_5 330K " "

+ = +300 volts

R_6 10K $\frac{1}{2}$ watt
 R_7 68K 2 "
 R_8 27K 1 "
 R_9 68K $\frac{1}{2}$ "
 R_{ij} See Section 3-3.

- = -300 volts

C_1 250pf
 C_2 0.15 f
 D_1 1N191
 V_1 5751 (12AX7)
 V_2 12AT7
 V_3 5651

Figure 3-4. Multivibrator and Gating Circuits.

$$V_1 + V_2 + \dots + V_k = 0).$$

A schematic of the output stage is shown in Figure 3-5.

The response of this network at time t

to a step input of V_i volts at time 0

$$\text{is } e_o(t) = -V_i \frac{R_o}{R_i} \left(1 - e^{-\frac{t}{\tau_o}}\right) \text{ where}$$

$$\tau_o = R_o C.$$

Similarly, the response at

time t to a step input of $\frac{1}{k} V_i$ volts

$$\text{at time 0 is } e_o(t) = \frac{-V_i}{k} \left(\frac{R_o}{R_i} \right) \left(1 - e^{-\frac{t}{\tau_o}}\right)$$

Regrouping gives,

$$e_o(t) = -V_i \left(\frac{R_o}{kR_i} \right) \left(1 - e^{-\frac{t}{\tau_o}}\right)$$

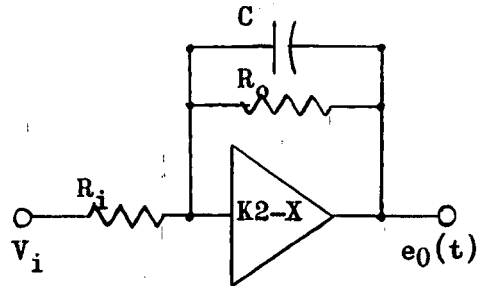


Figure 3-5. Output Network.

That is, by choosing values for V_i , R_i , R_o , and τ_o , then the input resistor value for an output scaled down (weighted) by a factor $\frac{1}{k}$ is just k times the unit resistor value R_i . In the noise generator, the V_i 's were chosen to be ± 45 volts, and the R_i 's were chosen to give output voltages weighted as described in the preceding paragraph.

The time-constant τ_o was chosen to be approximately equal to the duration of the voltage steps from the multivibrator chains. The value of the resistor R_o was chosen so that the maximum excursions of the smoothed waveform are ± 100 volts.

The values of the components are tabulated below with the steady-state output voltages and the output voltages at time τ_o .

Resistance	Steady-state voltage	Voltage at τ_0
$R_{11} = 60K$	- 51.0	- 32.5
$R_{12} = 90K$	+ 34.0	+ 21.7
$R_{13} = 180K$	+ 17.0	+ 10.8
$R_{21} = 75K$	+ 40.8	+ 26.0
$R_{22} = 100K$	- 30.6	- 19.5
$R_{23} = 150K$	- 20.4	- 13.0
$R_{29} = 300K$	+ 10.2	+ 6.5
$R_{31} = 84K$	+ 36.5	+ 23.2
$R_{32} = 120K$	- 25.5	- 16.3
$R_{33} = 160K$	- 19.1	- 12.2
$R_{34} = 210K$	+ 14.6	+ 9.3
$R_{35} = 480K$	- 6.4	- 4.1
$R_0 = 68K$	$C = 0.15 \mu f.$	$\tau_0 = 10.2 \text{ msec.}$

4. Analysis of the Noise Signal.

4-1. Introduction.

The analysis of the noise signal consisted of a theoretical and an experimental determination of the probability distribution of amplitudes and of the autocorrelation function of the signal. The methods of determination and the results so obtained are discussed in the following sections, as well as a comparison of the experimental and theoretical results.

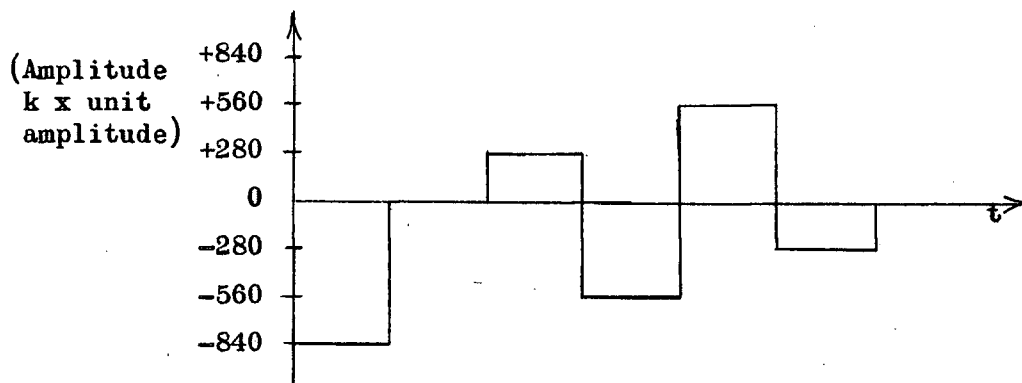
4-2. Theoretical Analysis

The theoretical analysis was not of the actual output signal, but rather of the unsmoothed output signal. Consequently, only a rough agreement with the experimental results was expected. The unsmoothed waveform was used as an approximation to the actual signal because it is composed of truly periodic functions and hence lends itself more readily to theoretical analysis than does the actual signal which is composed of aperiodic functions.

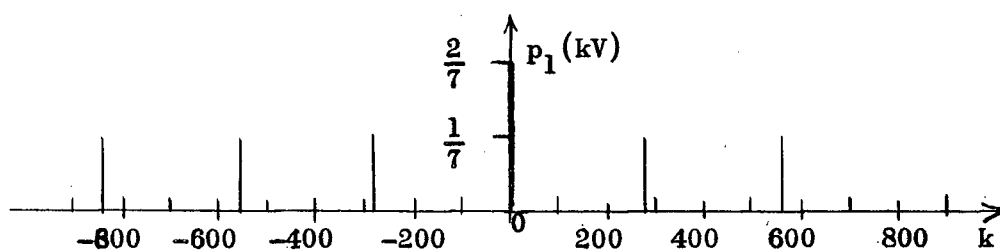
4-2-1. Theoretical Amplitude Probability Distribution.

The probability distribution of amplitudes was determined by considering the distribution obtained by sampling the waveform over a long time interval. To determine this distribution it is necessary to dissociate the unsmoothed signal into its component parts.

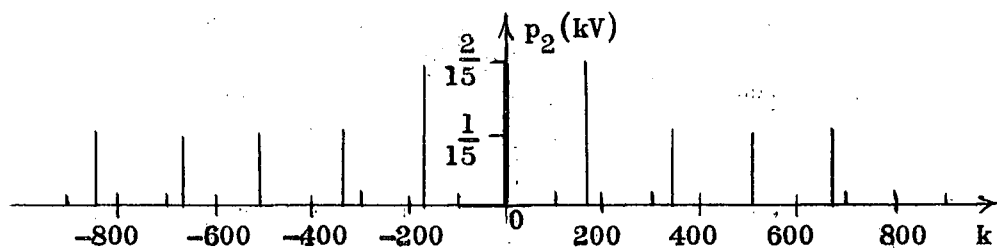
Consider first the waveform obtained from the first multi-vibrator chain. (Figure 4-1 (a)) If this waveform were sampled ran-



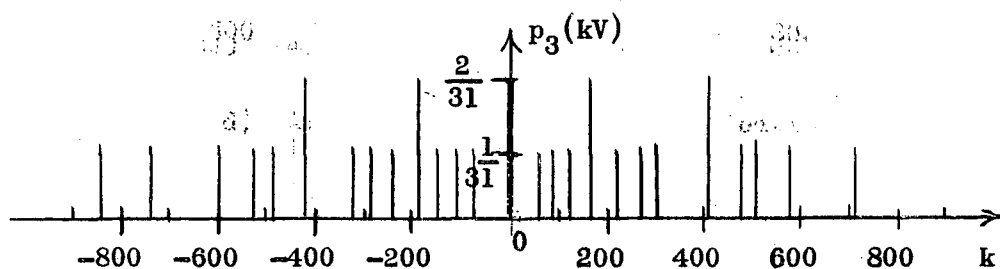
a) Waveform from Chain One.



b) Amplitude Probability Distribution
for Chain One Waveform.



c) Amplitude Probability Distribution
for Chain Two Waveform.



d) Amplitude Probability Distribution
for Chain Three Waveform.

Figure 4-1. Amplitude Probability Distributions.

domly over a large number of cycles of the waveform, the probability distribution of amplitudes would be as in Figure 4-1 (b). Similarly, for the second and third chains, the probability distributions of amplitudes would be as in Figure 4-1 (c) and Figure 4-1 (d) respectively. Thus, there is an average probability $p_1(k_1V)$ that a voltage k_1V is delivered by chain 1 at a time t , an average probability $p_2(k_2V)$ that a voltage k_2V is delivered by chain 2 at a time t , and an average probability $p_3(k_3V)$ that a voltage k_3V is delivered by chain 3 at a time t . Because the waveforms have non-multiple periods, in the average the cross-correlation between any two of the member functions is zero, and hence the average probabilities associated with the waveforms are independent. That is, the probability of occurrence of $V_o = (k_1 + k_2 + k_3)V$ is just the product of the individual probabilities. (i.e. $p(V_o) = p_1(k_1V)p_2(k_2V)p_3(k_3V)$.)

If we associate with each member function a generating function $G_i(s)$,⁸ we may easily determine the probability of occurrence of a certain output amplitude. For member function 1 we have

$$G_1(s) = \sum p_1(k_1V)s^{k_1}$$

$$= \frac{1}{7}s^{560} + \frac{1}{7}s^{280} + \frac{2}{7}s^0 + \frac{1}{7}s^{-280} + \frac{1}{7}s^{-560} + \frac{1}{7}s^{-840}$$

The coefficient of s^k is the probability of the voltage kV occurring.

There are similar generating functions $G_2(s)$ and $G_3(s)$ for member functions 2 and 3 respectively. (The powers of s are high because the unit voltage V was chosen so that all the k 's would be integers.)

Because the average probabilities associated with the member functions

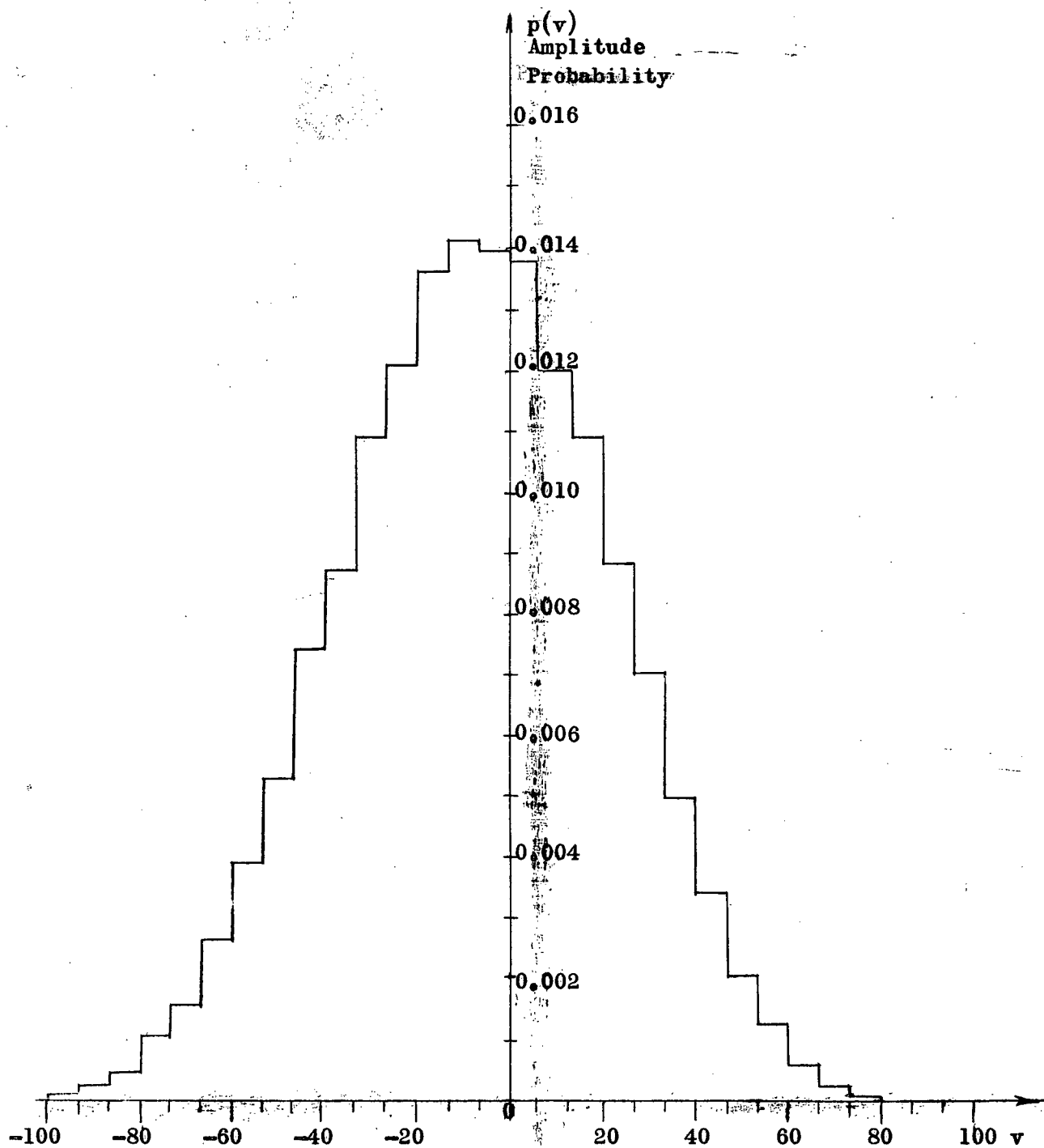


Figure 4-2. Theoretical Normalized Amplitude Probability Distribution.

are independent, the generating function for the sum of the waveforms is equal to the product of the generating functions of the individual waveforms, i.e. $G_0(s) = G_1(s)G_2(s)G_3(s)$. The product of the generating functions consists of about 3000 terms, and so a programme was written for the Alvac III E computer, (See Appendix B), to group the terms according to the values of the exponents and to count the number of terms whose exponents lie in the range $(n)168$ to $(n+1)168$. (i.e. $(n)168 \leq k < (n+1)168$, $n = -15, -14, \dots, 0, \dots, 15$.) Dividing the count for each range by $7(15)31$ gives the average probability that the output amplitude lies in the range $(n)168$ and $(n+1)168$, since the fraction so formed is the coefficient of the term $s^{(n)168}$. (The range 168V corresponds to an increment of $\frac{200}{31}$ volts = 6.45 v.) A plot of the normalized theoretical amplitude probability distribution is shown in Figure 4-2.

4-2-2. Theoretical Autocorrelation Function.

The autocorrelation function $\phi(\tau)$ of a function $F(t) = f_1(t) + f_2(t) + f_3(t)$, where $f_1(t)$, $f_2(t)$, and $f_3(t)$ are periodic functions with coprime periods, is merely the sum of the autocorrelation functions of the individual functions.²² This is because the multiplication of components of different frequencies results in a zero average value. In the case of a periodic waveform, the basic form of the autocorrelation function

$$\phi(\tau) = \lim_{T \rightarrow \infty} \frac{1}{2T} \int_{-T}^{+T} f(t) f(t + \tau) dt$$

may be replaced by the expression

$$\phi(\tau) = \frac{1}{\tau_j} \int_0^{\tau_j} f(t) f(t + \tau) dt$$

where $f(t)$ is periodic of period τ_j .

Consider a function $f(t)$ of period $N\tau_1$ such that:

$$\begin{aligned} f(t) &= f_0 & 0 \leq t < \tau_1 \\ &= f_1 & \tau_1 \leq t < 2\tau_1 \\ &= f_k & k\tau_1 \leq t < (k+1)\tau_1 \\ &= f_{N-1} & (N-1)\tau_1 \leq t < N\tau_1 \end{aligned}$$

where $f_0, f_1, \dots, f_k, \dots, f_{N-1}$ are constants. (See Figure 4-3).

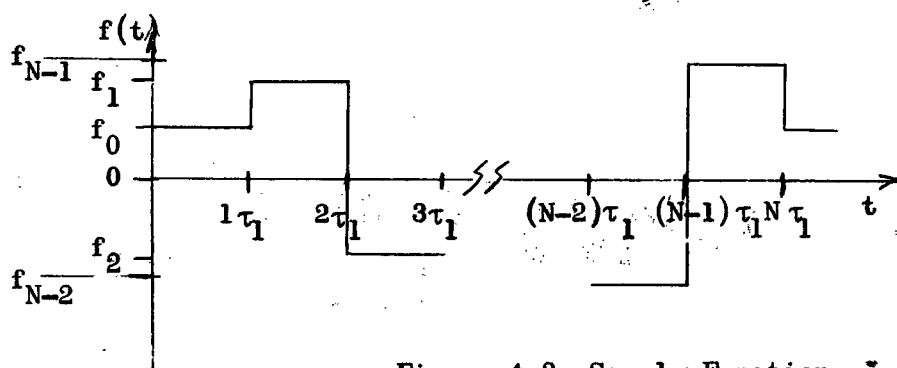


Figure 4-3. Sample Function.

The autocorrelation function $\phi(n\tau_1)$ is then,

$$\begin{aligned} \phi(n\tau_1) &= \frac{1}{N\tau_1} \int_0^{N\tau_1} f(t) f(t+n\tau_1) dt = \frac{1}{N\tau_1} \left(\int_0^{\tau_1} f(t) f(t+n\tau_1) dt + \right. \\ &+ \int_{\tau_1}^{2\tau_1} f(t) f(t+n\tau_1) dt + \dots + \int_{(N-1)\tau_1}^{N\tau_1} f(t) f(t+n\tau_1) dt \Big) = \\ &= \frac{1}{N\tau_1} \left(f_0 \int_0^{\tau_1} f(t+n\tau_1) dt + \dots + f_{N-1} \int_{(N-1)\tau_1}^{N\tau_1} f(t+n\tau_1) dt \right) = \\ &= \frac{1}{N\tau_1} \left(f_0 f_n \int_0^{\tau_1} dt + f_1 f_{n+1} \int_{\tau_1}^{2\tau_1} dt + \dots + f_{N-1} f_{N-1+n} \int_{(N-1)\tau_1}^{N\tau_1} dt \right) = \end{aligned}$$

$$= \frac{1}{N} (f_0 f_n + f_1 f_{n+1} + \dots + f_{N-1} f_{N-1+n})$$

Similarly we may write

$$\phi((n+1)\tau_1) = \frac{1}{N} (f_0 f_{n+1} + f_1 f_{n+2} + \dots + f_{N-1} f_{N+n})$$

Suppose, however, the time-shift is not an integral number times τ_1

but, say $(n+\alpha)\tau_1$ where $0 \leq \alpha < 1$.

$$\begin{aligned} \text{Then, } \phi((n+\alpha)\tau_1) &= \frac{1}{N\tau_1} \int_0^{N\tau_1} f(t) f(t+(n+\alpha)\tau_1) dt = \\ &= \frac{1}{N\tau_1} (f_0 \int_0^{\tau_1} f(t+(n+\alpha)\tau_1) dt + \dots + f_k \int_{k\tau_1}^{(k+1)\tau_1} f(t+(n+\alpha)\tau_1) dt + \dots \\ &\quad + f_{(N-1)} \int_{(N-1)\tau_1}^{N\tau_1} f(t+(n+\alpha)\tau_1) dt) \end{aligned}$$

Consider the general term in the bracket, $f_k \int_{k\tau_1}^{(k+1)\tau_1} f(t+(n+\alpha)\tau_1) dt$.

Now, $f(t+(n+\alpha)\tau_1)$ assumes two values in the range $k\tau_1 \leq t \leq (k+1)\tau_1$.

For $k\tau_1 \leq t \leq k\tau_1 + (1-\alpha)\tau_1$ we have $f(t+(n+\alpha)\tau_1) = f_{k+n}$ and for

$k\tau_1 + (1-\alpha)\tau_1 \leq t \leq (k+1)\tau_1$ we have $f(t+(n+\alpha)\tau_1) = f_{k+n+1}$. There-

fore, the integral $\int_{k\tau_1}^{(k+1)\tau_1} f(t+(n+\alpha)\tau_1) dt$ equals

$$\int_{k\tau_1}^{(k+(1-\alpha))\tau_1} f_{k+n} dt + \int_{(k+(1-\alpha))\tau_1}^{(k+1)\tau_1} f_{k+n+1} dt = f_{k+n} (1-\alpha)\tau_1 + f_{k+n+1} \alpha\tau_1$$

and so the function $\phi((n+\alpha)\tau_1)$ becomes

$$\phi((n+\alpha)\tau_1) = \frac{1}{N\tau_1} (f_0 f_n (1-\alpha)\tau_1 + f_0 f_{n+1} \alpha\tau_1 + \dots$$

$$+ f_k f_{k+n} (1-\alpha) \tau_1 + f_k f_{k+n+1} (\alpha) \tau_1 + \dots + f_{N-1} f_{N+n-1} (1-\alpha) \tau_1 + \\ + f_{N-1} f_{N+n} (\alpha) \tau_1).$$

Regrouping and cancelling gives:

$$\phi((n+\alpha)\tau_1) = \frac{1}{N} (f_0 f_n + f_1 f_{n+1} + \dots + f_{N-1} f_{N+n-1}) + \\ + \frac{\alpha}{N} (f_0 f_{n+1} + f_1 f_{n+2} + \dots + f_{N-1} f_{N+n} - f_0 f_n - f_0 f_{n+1} - \dots \\ - f_{N-1} f_{N+n-1}) = \phi(n\tau_1) + \alpha (\phi((n+1)\tau_1) - \phi(n\tau_1))$$

Thus, the autocorrelation function of this rectangular-shaped waveform is a triangular-shaped function having the same period as the original function. The autocorrelation function $\phi(\tau)$ is an even function and hence $\phi(\tau) = \phi(-\tau)$. But, $\phi(\tau) = \phi(N\tau_1 + \tau)$ and also $\phi(-\tau) = \phi(N\tau_1 - \tau)$. Therefore, $\phi(\tau) = \phi(N\tau_1 - \tau)$.

That is, the autocorrelation function is symmetric about the half-period point $\frac{N\tau_1}{2}$. A plot of the normalized theoretical autocorrelation functions $\frac{\phi_{11}(\tau)}{\phi_{11}(0)}$, $\frac{\phi_{22}(\tau)}{\phi_{22}(0)}$, and $\frac{\phi_{33}(\tau)}{\phi_{33}(0)}$ for the member functions f_1 , f_2 , and f_3 are shown in Figures 4-4 (a), (b) and (c) respectively. (A programme was written to determine the cardinal points $\phi(n\tau_1)$. This programme is described in Appendix C.)

Because the individual waveforms have independent probability functions (i.e. are uncorrelated) the autocorrelation function of the sum of the waveforms is equal to the sum of the autocorrelation functions of the individual waveforms - that is,

$$\phi(\tau) = \phi_{11}(\tau) + \phi_{22}(\tau) + \phi_{33}(\tau), \text{ where } F(t) = f_1(t) + f_2(t) + f_3(t)$$

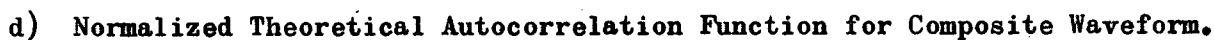
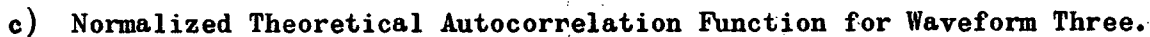
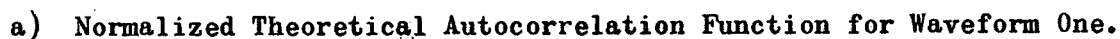


Figure 4-4. Theoretical Normalized Autocorrelation Functions.

and $\phi(\tau)$ is the autocorrelation function of $F(t)$. The normalized autocorrelation function of the composite waveform is

$$\frac{\phi(\tau)}{\phi(0)} = \frac{\phi_{11}(\tau) + \phi_{22}(\tau) + \phi_{33}(\tau)}{\phi_{11}(0) + \phi_{22}(0) + \phi_{33}(0)}$$

A plot of the normalized autocorrelation function $\frac{\phi(\tau)}{\phi(0)}$ is shown in Figure 4-4 (d).

4-3. Experimental Analysis.

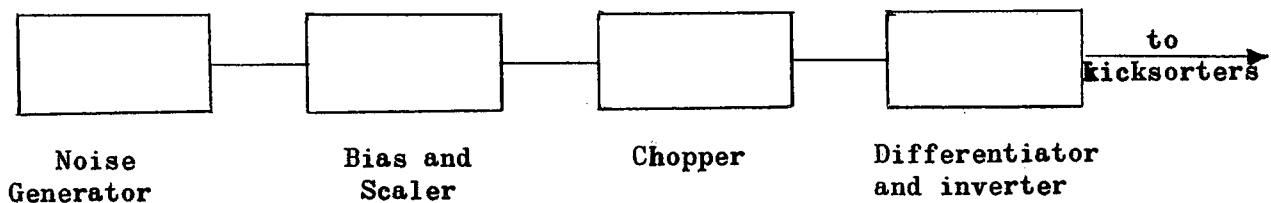
A laboratory determination was made of the amplitude probability distribution and of the autocorrelation function of the actual output signal. The probability distribution of amplitudes was determined using sampling techniques and the autocorrelation function was determined using two of the noise generators and a multiplying and averaging device. These methods are described in the following sections.

4-3-1. Experimental Amplitude Probability Distribution.

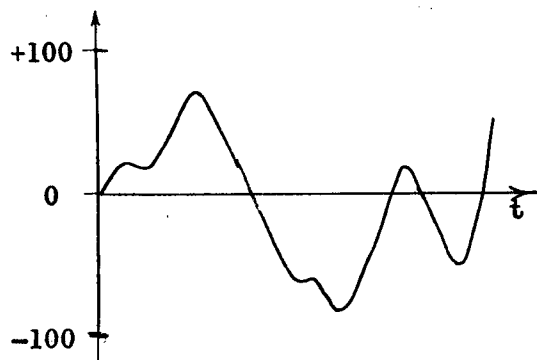
The method by which the amplitude probability distribution was obtained was to sample the waveform 500 times per second for a time T_n minutes, and to count the number of times the amplitude of the pulse so formed was in the range v to $v + \Delta v$. Dividing this number by the total number of pulses then gives the probability of the amplitude of the waveform lying in the range v to $v + \Delta v$. The time T_n was chosen because this is the near-period of the signal and hence should give an accurate probability distribution for all time intervals. The sampling frequency

(500 times per second) was chosen to be very much higher than the half-power bandwidth of the noise signal (approximately 16 cps as determined by τ_0 , the smoothing-network time-constant) so that, in effect, the waveform was sampled continually and consequently the count for a particular amplitude is a very accurate measure of the time the waveform was at that amplitude during the time T_n . A block diagram of the sampling system is shown in Figure 4-5 (a), and the waveforms at various points in the sampling process are shown in Figure 4-5 (b). The chopper system consisted of a gating circuit activated by a bistable multivibrator. The differentiator and inverter system consisted of a Philbrick K2-X unit²⁰ which inverted the chopped waveform, followed by a simple RC differentiating network. The K2-X unit was used so as to provide a high-impedance resistive load for the gating circuit and to allow a gain adjustment to offset the slight attenuation introduced by the differentiating network. Thus, the amplitude of the pulse delivered at time t by the differentiating network may be made exactly equal to the instantaneous amplitude of the noise signal at the time t . The circuit diagrams for the chopper and differentiator units are shown in Figure 4-6.

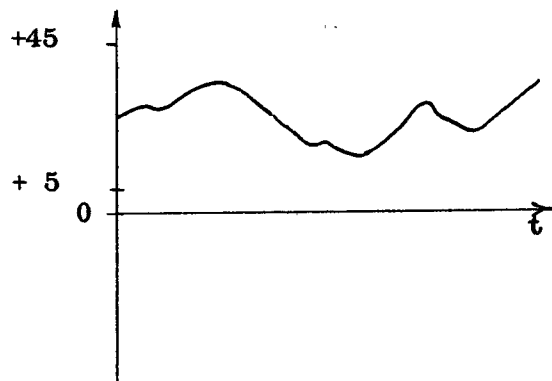
The pulse-height discriminators (kicksorters) used were Marconi type 115-935, and were the property of the Van de Graaff section of the U.B.C. Physics Department. Thirty kicksorters were available and so it was possible to divide the noise signal into 30 discrete amplitude ranges, 0 to V_1 , V_1 to V_2 , ..., V_{29} to V_{30} , and so determine the number of counts for each range. The maximum



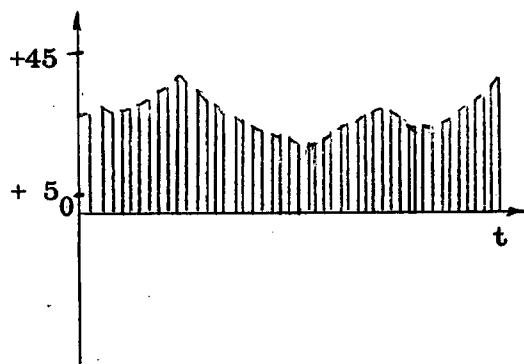
a) Block Diagram of Sampling System.



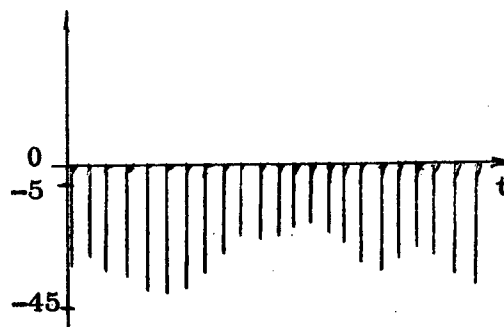
Output of Noise Generator



Output of Bias and Scaler



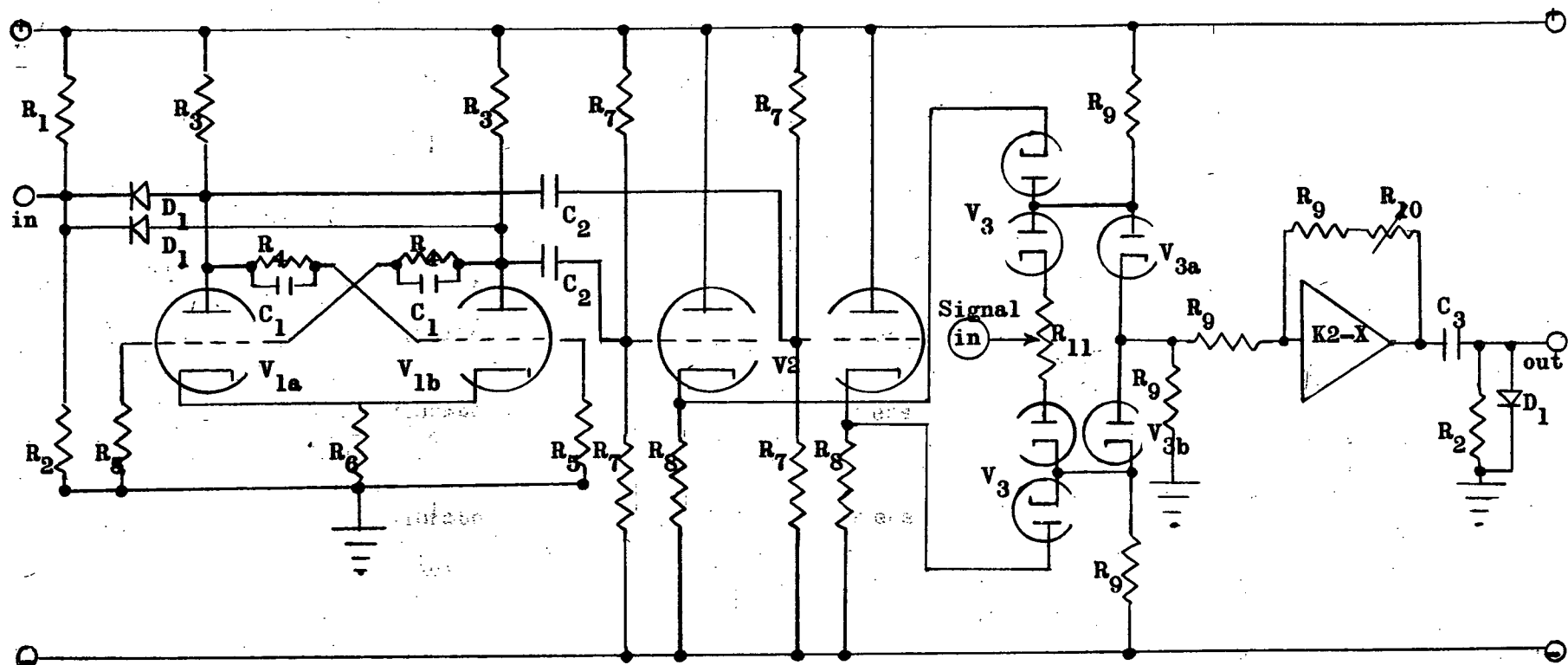
Output of Chopper



Output of Differentiator and inverter

b) Waveforms in Sampling System.

Figure 4-5. Sampling System Schematic.



Bistable Multivibrator

R ₁ 33K	1/2 watt
R ₂ 100K	" "
R ₃ 15K	1 "
R ₄ 47K	1/2 "
R ₅ 4.7K	" "
R ₆ 2.2K	1 "

Cathode Followers

R ₇ 2.2MEG	1/2 watt
R ₈ 150K	" "
R ₉ 1MEG	" "
R ₁₀ 50K	" " pot.
C ₁ 500pf	" "
C ₂ 0.01μf	" "

Diode Gates

C ₃ 250pf
V ₁ 12AT7
V ₂ 12AX7
V ₃ 6AL5
D ₁ 1N191
R ₁₁ 1K pot.

Differentiating Circuit

+ = +300 volts

- = -300 volts

Figure 4-6. Chopper and Differentiator Circuit.

pulse amplitude accepted by the kicksorters was 40 volts (negative-going) and the maximum counting rate per channel was 50 pps for sustained counting.¹⁶ For this reason, the noise signal was scaled down and biased so that the maximum signal excursions were from +5 to +45 volts. The pulses delivered from the inverter and differentiator system thus had an amplitude of from -5 to -45 volts. The noise signal was made to vary from +5 to +45 volts so that the minimum pulse amplitude due to the signal (i.e. 5 volts) was greater than the maximum pulse amplitude caused by switching transients in the chopper system, (approximately 2 volts). Because the maximum allowed counting rate was only 50 pps, it was necessary to make the voltage ranges $\Delta V_i = V_i - V_{i+1}$ ($i = 1, 2, \dots, 30$) of different magnitudes in order to obtain an accurate count of the number of pulses of each amplitude. Using the theoretical probability distribution of amplitudes as a guide, a set of values was determined for the V_i 's so as to ensure the counting of all the pulses. The normalized probability distribution obtained from the kicksorter data is shown in Figure 4-7.

4-3-2. Experimental Autocorrelation Function.

The experimental autocorrelation function was obtained by using two of the noise generators and a multiplier and an integrator. Generator one was turned on a time τ before generator two, and the signals $N(t)$ and $N(t + \tau)$ were multiplied and integrated for a period of six minutes and fifteen seconds (almost the near-period duration). Dividing the value of the integrator count obtained for the time

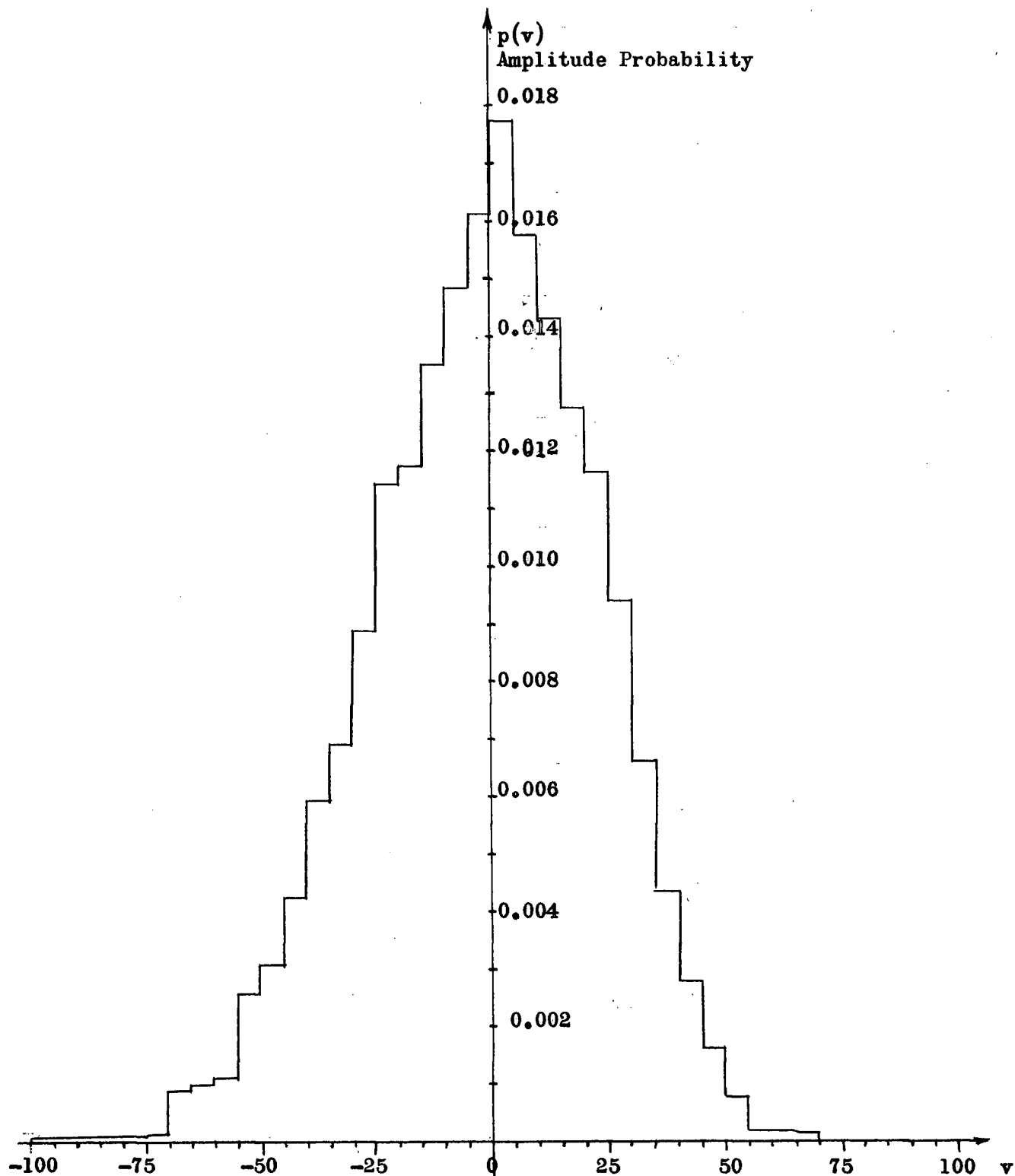


Figure 4-7. Experimental Normalized Amplitude Probability Distribution.

shift τ by the value of the integrator count obtained for the time shift of 0 seconds gives the normalized autocorrelation function for that particular value of τ . Shifts of 30 seconds were made for the range $\tau = 0$ to $\tau =$ six minutes, and the resulting values of the autocorrelation function are shown plotted in Figure 4-8.

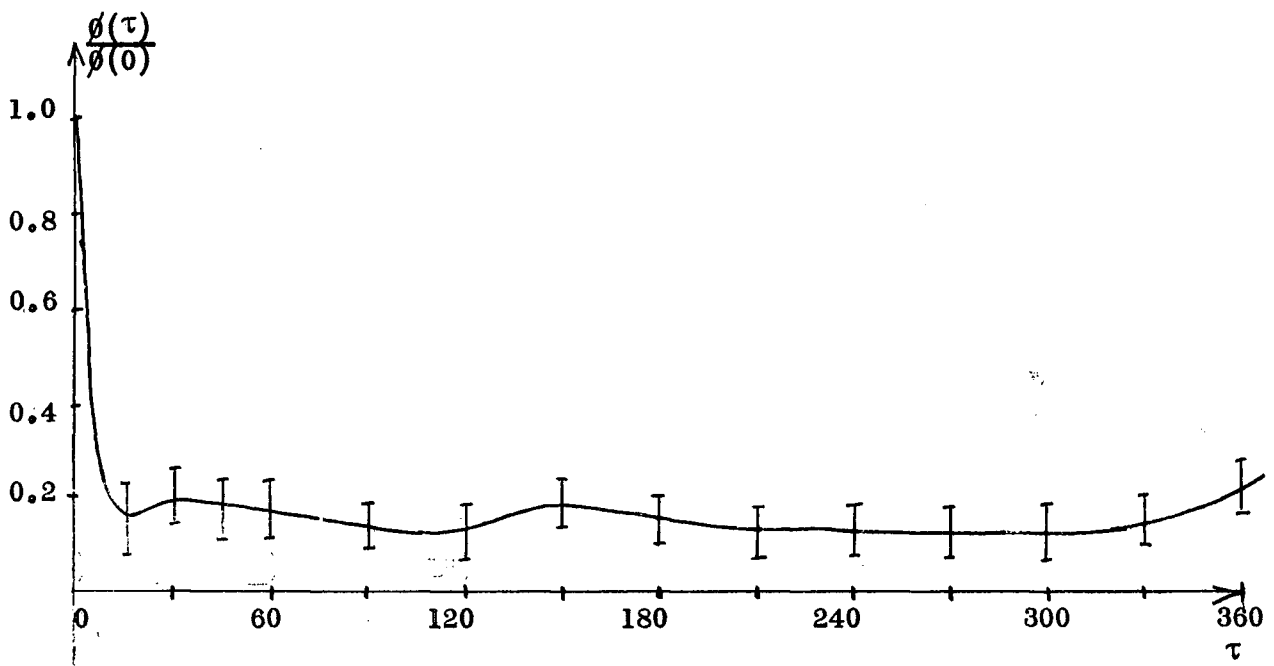


Figure 4-8. Experimental Normalized Autocorrelation Function.

The multiplier used was a Philbrick Model MU/DV Duplex Multiplier/Divider.²⁰ The output from each generator was scaled down so that the maximum signal excursions at the input and output of the multiplier were in the allowed range of ± 50 volts. The output of the multiplier was then scaled down and fed into an ac tachometer-feedback servo motor. The speed of the motor was proportional to the voltage in and hence the count of the number of revolutions of the motor for a given time T_n represents the integral of the speed

for that time (i.e., the count is proportional to the value of the integral of the input voltage for the time T_n). Since a normalized autocorrelation function was desired, it was only necessary to ascertain over what range of input voltages the integrator was linear, and then keep within that range. The constant of proportionality cancels out in the normalization procedure. A block diagram of the correlator is shown in Figure 4-9 and the circuit diagram for the integrator is shown in Figure 4-10.

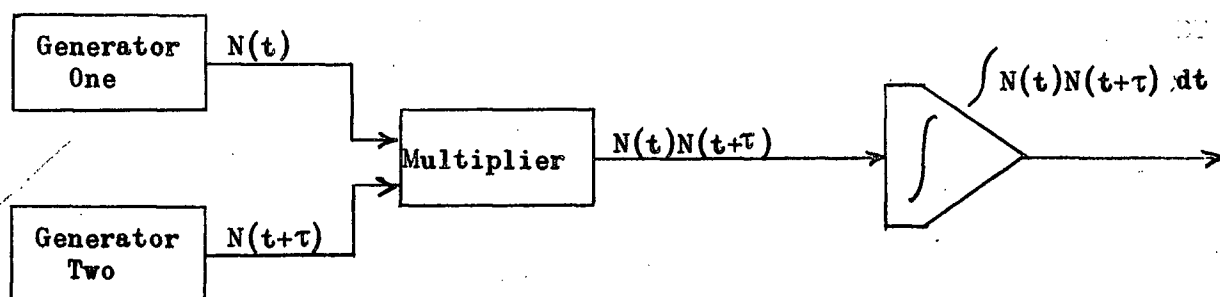


Figure 4-9. Block Diagram of Correlator.

4-4. Comparison of Theoretical and Experimental Results.

The theoretical and experimental amplitude probability distributions and a computed Gaussian distribution are shown together in Figure 4-11. The Gaussian curve was computed using the mean and mean-square values calculated from the experimental distribution. A very good fit was obtained. The theoretical distribution was shifted to the right (13.5 - 2.1) volts = 11.4 volts so as to make the theoretical and experimental means coincide. As was expected, the experimental distribution was more peaked near zero amplitude than was the theoretical distribution. This is due to the action

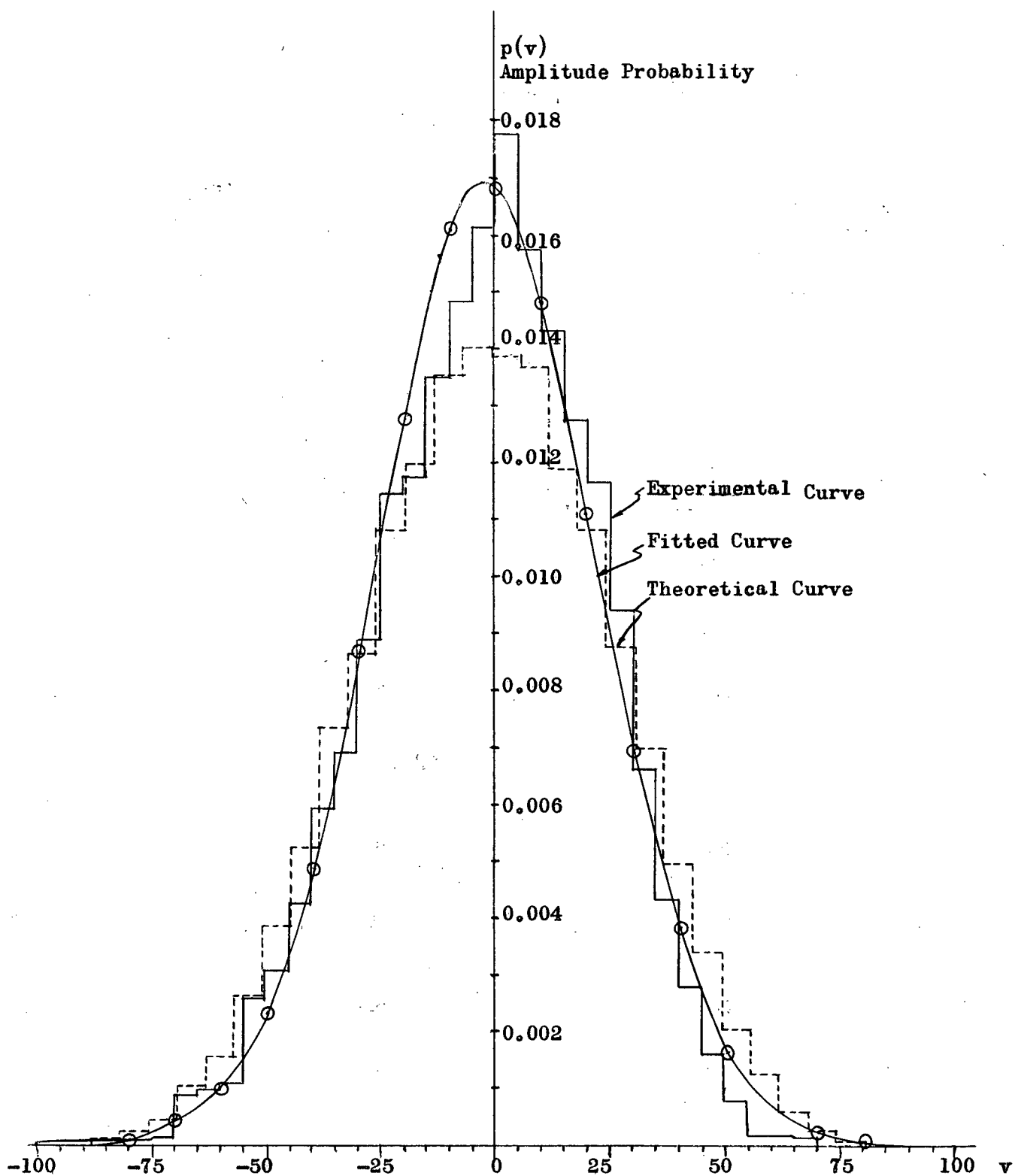


Figure 4-11. Normalized Probability Distributions.

of the smoothing network in the output stage of the generator. The good Gaussian fit may be justified by viewing the generation process of the noise signal in a slightly different manner - viz., consider the noise signal as being generated by adding many short pulses of various amplitudes and of various durations. (See Figure 4-12.). The Central Limit Theorem of statistics³ provides the means for justification. This theorem states that the distribution of the sum of an indefinitely large number of other independently distributed quantities must approach the Gaussian distribution, no matter what the individual distributions may be.

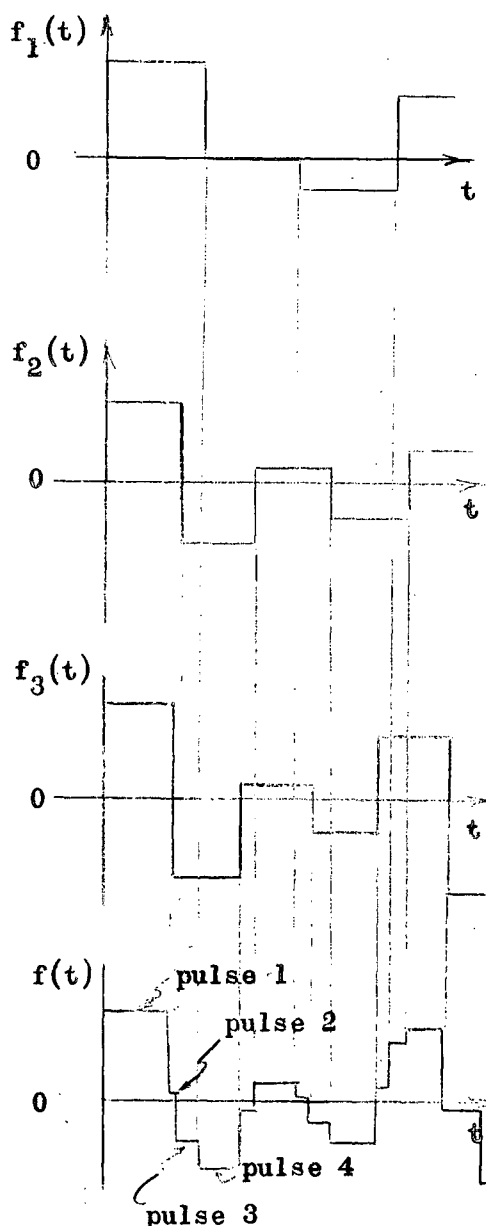


Figure 4-12. Alternate Form of Dissociation of Noise Signal.

The theoretical and experimental autocorrelation functions for the noise signal are shown in Figure 4-13. Poor agreement between the two results was expected because no account was taken of the smoothing network effects in the theoretical determination, and also

the accuracy of the integrator is questionable. (It is proposed to build a precision dc tachometer-feedback servo integrator in order to more accurately determine the autocorrelation function.) The experimental and theoretical results agree very well, however, under the circumstances.

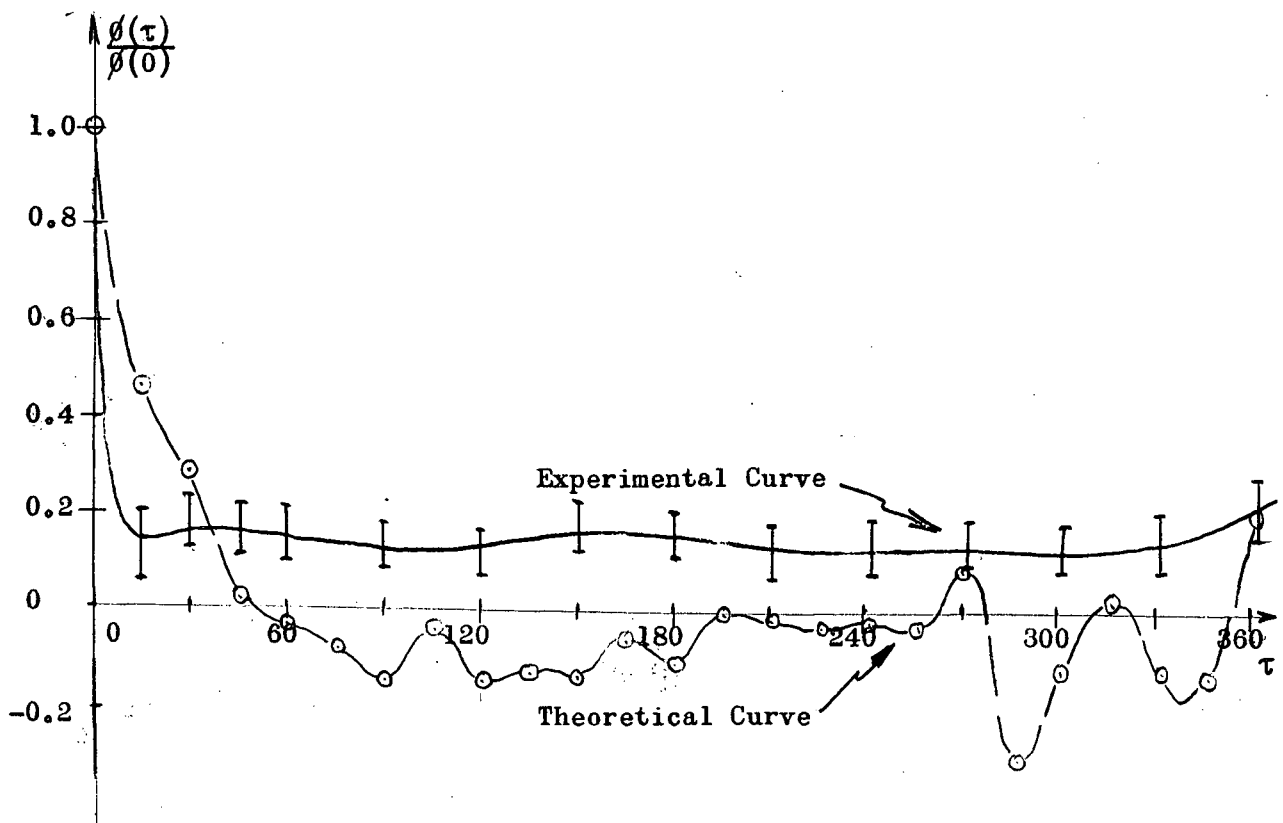


Figure 4-13. Theoretical and Experimental Autocorrelation Functions.

5. Conclusions.

Examination of the data obtained fails to reveal a precise relationship between the theoretical and experimental probability distributions. The general good agreement between the theoretical and experimental results does, however, attest to the validity of the theoretical analyses of the waveforms. On this basis, it is suggested that the noise signal produced using the initial configurations of the multivibrators as described in Case 2, Appendix B, would have a more nearly Gaussian probability distribution of amplitudes. This is because the signal so generated would be composed of member functions which are balanced (i.e. have equal positive and negative voltage steps).

A determination of the power spectrum of the signal would be of help in ascertaining if the signal is a true noise signal (or nearly so) and also would specify the bandwidth of the noise signal. The signal probably has a bandwidth of 0 to 60 cps (approximately). This figure was arrived at from visual examination of the output of the sampling system when the sampling frequency was varied from 500 cps down to 20 cps. At a sampling frequency of 100 cps there were very abrupt changes in the output of the sampling system. This indicates that considerable change in the noise signal had taken place in the time between samples. This would occur if the noise signal had a frequency component of around 50 cps.

On the basis of tests and observations made, it is con-

cluded that the signal generated may be considered a noise signal having a near-Gaussian amplitude probability distribution, very little correlation for time-shifts greater than 30 seconds, and a bandwidth of about 60 cps.

Appendix A.

A-1. Programme for Determining the Near-periods of a Function.

As developed in the text (Section 2-3-2) the problem involved in determining the near-periods of a composite function may be stated mathematically as: Given integers δ , K , L , and M , determine integers x , y , and z so that $|zM-xK| \leq \delta$, $|zM-yL| \leq \delta$, and $|xK-yL| \leq \delta$. A brief explanation of the programme used to determine the integers x , y , and z for a given set of K , L , and M is presented in the next paragraph.

An augmenting procedure is used in this programme. The computer takes a value of z (say z_n) and calculates the two integers x_{n1} (below) and x_{n2} (above) nearest to the value $x_n = \frac{z_n M}{K}$. The machine then tests to see if $|z_n M - x_{n1} K| \leq \delta$ or if $|z_n M - x_{n2} K| \leq \delta$. If neither of x_{n1} nor x_{n2} satisfy the inequalities above, the cycle is repeated with z_n increased by 1. The initial value of z_n is 1 and so all values of z from 1 up are tried. This procedure continues until values of x and z are found (say x' and z') such that $|z' M - x' K| \leq \delta$. The machine then takes this value of z and computes the two integers y_1' (below) and y_2' (above) nearest to $y' = \frac{z' M}{L}$. The machine then tests to see if either $|z' M - y_1' L| \leq \delta$ or $|z' M - y_2' L| \leq \delta$. If neither y_1' nor y_2' satisfy these inequalities, the computer returns to the beginning of the programme and starts to determine new values of x and z , this time with the initial value of $z_n = z' + 1$.

This series of calculations and decisions is continued until values of x , y , and z are found which satisfy $|zM-xK| \leq \delta$ and

$|z_M - y_L| \leq \delta$. The machine then outputs $(z_M - x_K)$, $(z_M - y_L)$, $(x_K - y_L)$, x , y , and z and then returns to the beginning of the programme where it starts to determine new values of x and z , this time with the initial value of $z_n = z + 1$. The programme continues until the operator stops the machine. A copy of the programme tape is given below.

```
a004
83a15717 2c006720 1d967926 112c0000
2800f1c6 1d8d791f 67224926 7934f781
48241107 611b491f 2c006720 1704110c
411fe723 110c7928 1d121185 00000000
eb21c528 611b4928 7929611b 00000000
49256720 411fe723 4929791f 00040000
1d157925 eb22c529 492a7926 00000001
67214925 49266720 67254927 00000001
```

```
a104
00000000 00000000 00000000 00000000
00000000 00000000 00000000 00000000
00000000 00000000 00000000 00000000
7934f781 17341185 58000000 00000000
5732871f 00000000 00060000 00000000
5b36782b 00000000 050000b8 00000000
1160792e 00000000 00000000 00000000
f781112d 00000000 00000000 00000000
2822
a0 61750ec2
a1 a8b99365
```

A-2. Computer Results

A partial list of the results for the case $\delta = 600$, $K = 14850$, $L = 7280$, and $M = 29760$ is presented below.

(zM-xK)	(zM-yL)	(xK-yL)	x	y	z
-570	-560	010	477	973	238
-510	080	590	479	977	239
150	-160	-310	501	1022	250
210	480	270	503	1026	251
-360	-080	280	980	1999	489
360	320	-040	1004	2048	501
-210	-240	-030	1481	3021	739
-150	400	550	1483	3025	740
510	160	-350	1505	3070	751
-060	-400	-340	1982	4043	989
000	240	240	1984	4047	990
-570	-320	250	2461	5020	1228
150	080	-070	2485	5069	1240

The value of δ used in this case corresponds to a time of

$\delta T = 6.0$ msecs. The time between pulses into the chains is approximately the same for all the chains and is about 10 msecs. Thus, the value of δT corresponds to about half the time between pulses into the chains. All the values of the differences were felt to be great enough to cause sufficient change in the composite waveform up to the value of $x = 2485$. At this point, the maximum shift of any one of the member functions with respect to the others is only 1.5 msecs which was considered too small to cause sufficient change in the composite waveform. Thus, this value of x determines the near-period of the waveform. The near-period is $T_n = \frac{(14850)2485}{100,000}$ secs = 369.0225 secs which is approximately six minutes.

Appendix B

B-1. Programme for Determining the Theoretical Probability Distribution of Amplitudes.

To determine the theoretical probability distribution of amplitudes, it was necessary to find the product of the generating functions of the individual waveforms. Each generating function is a polynomial in s and is of the general form $G(s) = \sum_k p(kV)s^k$, where $p(kV)$ is the probability of the amplitude kV occurring. For example, the generating function $G_1(s)$ for waveform 1 is:

$G_1(s) = \frac{1}{7} s^{560} + \frac{1}{7} s^{280} + \frac{2}{7} s^0 + \frac{1}{7} s^{-280} + \frac{1}{7} s^{-560} + \frac{1}{7} s^{-840}$, which consists of 6 terms. This may be written as 7 terms, each having the coefficient $\frac{1}{7}$, which may be factored out. This gives,

$$G_1(s) = \frac{1}{7} (s^{560} + s^{280} + s^0 + s^0 + s^{-280} + s^{-560} + s^{-840}).$$

Similarly, $G_2(s)$ and $G_3(s)$ may be written: $G_2(s) = \frac{1}{15} (\dots 15 \text{ terms in } s^k \dots)$ and $G_3(s) = \frac{1}{31} (\dots 31 \text{ terms in } s^k \dots)$. If now the product of these polynomials is formed, the result would be of the form $G(s) = \frac{1}{7(15)31} (\dots 7(15)31 \text{ terms in } s^k \dots)$. The values of the exponents in this expression are obtained by taking the sum of all possible combinations of the 7 exponents from $G_1(s)$ plus the 15 exponents from $G_2(s)$ plus the 31 exponents from $G_3(s)$, a total of $7(15)31 = 3255$ sums. The generating function so formed is of the same form as the modified version of $G_1(s)$ (above). Multiplying each term by the common factor $\frac{1}{3255}$ and grouping together the terms having the same value of the exponent restores the generating function to the original form. (i.e. $G(s) = \sum_k p(kV)s^k$).

The coefficient of s^k (some multiple of $\frac{1}{3255}$) is then $p(kV)$, the probability of the amplitude kV occurring. Thus, when the number of times the exponent k occurs is known, the probability $p(kV)$ for the amplitude kV occurring is simply this number multiplied by $\frac{1}{3255}$. Because a quantized probability distribution was desired, it was sufficient to determine the number of times (say n_i) the exponent k was in the range k_i to k_{i+1} to get the probability that the amplitude was in the range $k_i V$ to $k_{i+1} V$.

A programme was written which calculated the sums of all possible combinations of 7 plus 15 plus 31 numbers and counted the total number of times the sums lay in each of 31 equal ranges. The 7, 15, and 31 numbers to be summed were all positive. (This merely means removing the factor s^{-840} from the generating functions and hence increasing the exponents in the brackets by 840.) The range of kV from -100 to +100 volts in the physical system corresponds to the range of k from 0 to 5040 in the computer. This range was divided into 31 equal increments of 168 units each, (which corresponds to dividing the range -100 to +100 v into 6.45 volt increments). The count for the range $(n(168))$ to $(n(168) + 167)$ $n = 0, 1, \dots, 30$ was stored in word location n in the computer. Thus, it was only necessary to divide the sum for a particular combination by 168 to determine the location of the count which should be increased by 1. A copy of the programme tape is given on the following page.

a004

```

573f2800 a5104927 4da67900 781f1160
f1c44847 793ba510 612f4900 00000000
17a0573b 491f7947 17b1791f 04000059
2800f1c4 6140497f 672f491f 00000001
4856172c 5737797f 19587927 000000a8
57372800 607f3000 672f4927 001f0000
f1c4487f 2800eb33 19565737 000f0000
17b4793f 30004da2 871f5b2b 00070000

```

a104

```

81a283a0 00000000 00000000 00000000
11200000 00000000 00000000 00000000
00000000 00000000 00000000 00000000
00000000 00000000 00000000 00000000
00000000 00000000 00000000 00000000
00000000 00000000 00000000 00000000
00000000 00000000 792fa710 4da91125
792f6129 795ff781 612d492d 00000000
492911a9 17be1120 6da41157 58000000

```

a204

```

00000000 00000000 00000000 00000000
00000000 00000000 00000000 00000000
00000000 00000000 00000000 00000000
00000000 00000000 00000000 00000000
00000000 00000000 00000000 00000000
00000000 00000000 00000000 00000000
00000000 00000000 00000000 00000000
00000000 00000000 00000000 00000000

```

2822

```

a0 d51658d9
a1 d3e311cf
a2 00000000

```

B-2. Computer Results.

Two determinations of probability distributions were made, each one corresponding to a different set of member functions. (Which in turn corresponds to a different initial configurations of the multivibrators in the multivibrator chains.) The waveform voltages for the two cases are tabulated for each member function set, where $V(n\tau_i)$ is the voltage step from the i^{th} chain after n pulses.

Case 1. (All multivibrators initially in the state where the output voltage is initially 0.) This was the case used in the generator.

Waveform 1.

$V(n\tau_1)=$	-840V	000V	+280V	-560V	+560V	-280V	000V
$n =$	1	2	3	4	5	6	7

Waveform 2.

$V(n\tau_2)=$	+168V	-504V	+336V	-336V	-168V	-840V	+168V	+336V
$n =$	1	2	3	4	5	6	7	8

$V(n\tau_2)=$	-336V	+504V	-168V	000V	-672V	+672V	000V
$n =$	9	10	11	12	13	14	15

Waveform 3.

$V(n\tau_3)=$	+180V	-420V	+285V	-315V	-135V	-735V	+735V	+135V
$n =$	1	2	3	4	5	6	7	8

$V(n\tau_3)=$	+315V	-285V	+420V	-180V	000V	-600V	+495V	-105V
$n =$	9	10	11	12	13	14	15	16

Waveform 3. (Continued)

$V(n \tau_3)$	=	+075V	-525V	+180V	-420V	-240V	-840V	+240V	+420V
n	=	17	18	19	20	21	22	23	24
$V(n \tau_3)$	=	-180V	+525V	-075V	+105V	-495V	+600V	000V	
n	=	25	26	27	28	29	30	31	

Case 2. (Multivibrators gating positive voltages in 0 state, multivibrators gating negative voltages in 1 state. This results in a symmetric waveform from each chain.)

Waveform 1.

$V(n \tau_1)$	=	-840V	+560V	-280V	+280V	-560V	+840V	000V
n	=	1	2	3	4	5	6	7

Waveform 2.

$V(n \tau_2)$	=	+672V	-504V	+168V	-336V	+336V	-840V	-168V	+168V
n	=	1	2	3	4	5	6	7	8
$V(n \tau_2)$	=	+840V	-336V	+336V	-168V	+504V	-672V	000V	
n	=	9	10	11	12	13	14	15	

Waveform 3.

$V(n \tau_3)$	=	+600V	-420V	+180V	-315V	+285V	-735V	-135V	+240V
n	=	1	2	3	4	5	6	7	8
$V(n \tau_3)$	=	+840V	-180V	+420V	-075V	+525V	-495V	+105V	-105V
n	=	9	10	11	12	13	14	15	16

Waveform 3. (Continued)

$V(n \tau_3) =$	+495V	-525V	+075V	-420V	+180V	-840V	-240V	+135V
$n =$	17	18	19	20	21	22	23	24

$V(n \tau_3) =$	+735V	-285V	+315V	-180V	+420V	-600V	000V
$n =$	25	26	27	28	29	30	31

A plot of the probability distributions obtained for each case is shown in Figure B-1. The shift in the mean values results because the member functions for the first case do not have equal numbers of positive and negative voltage steps whereas in the second case they do. This is also the reason why the curve for the second case is symmetric and that for the first case is not.

The relationship between the normalized probability distribution and the number of counts per range is given by the formula $p(kV) = \frac{C_k}{C_T \Delta V}$ where $p(kV)$ is the probability that the amplitude lies in the range $k\Delta V$ to $(k+1)\Delta V$, C_k is the number of counts for the range $(k(168) \text{ to } (k+1)168-1)$, and C_T is the total number of counts (i.e. $C_T = \sum C_k$).

The counts for each range are tabulated below for each case.

Case 1.

$C_n =$	2	5	9	21	32	53	79	107	149	176	220
$n =$	0	1	2	3	4	5	6	7	8	9	10

$C_n =$	244	275	286	282	278	242	220	178	142	101	69
$n =$	11	12	13	14	15	16	17	18	19	20	21

$C_n =$	42	25	12	5	1	0	0	0	0
$n =$	22	23	24	25	26	27	28	29	30

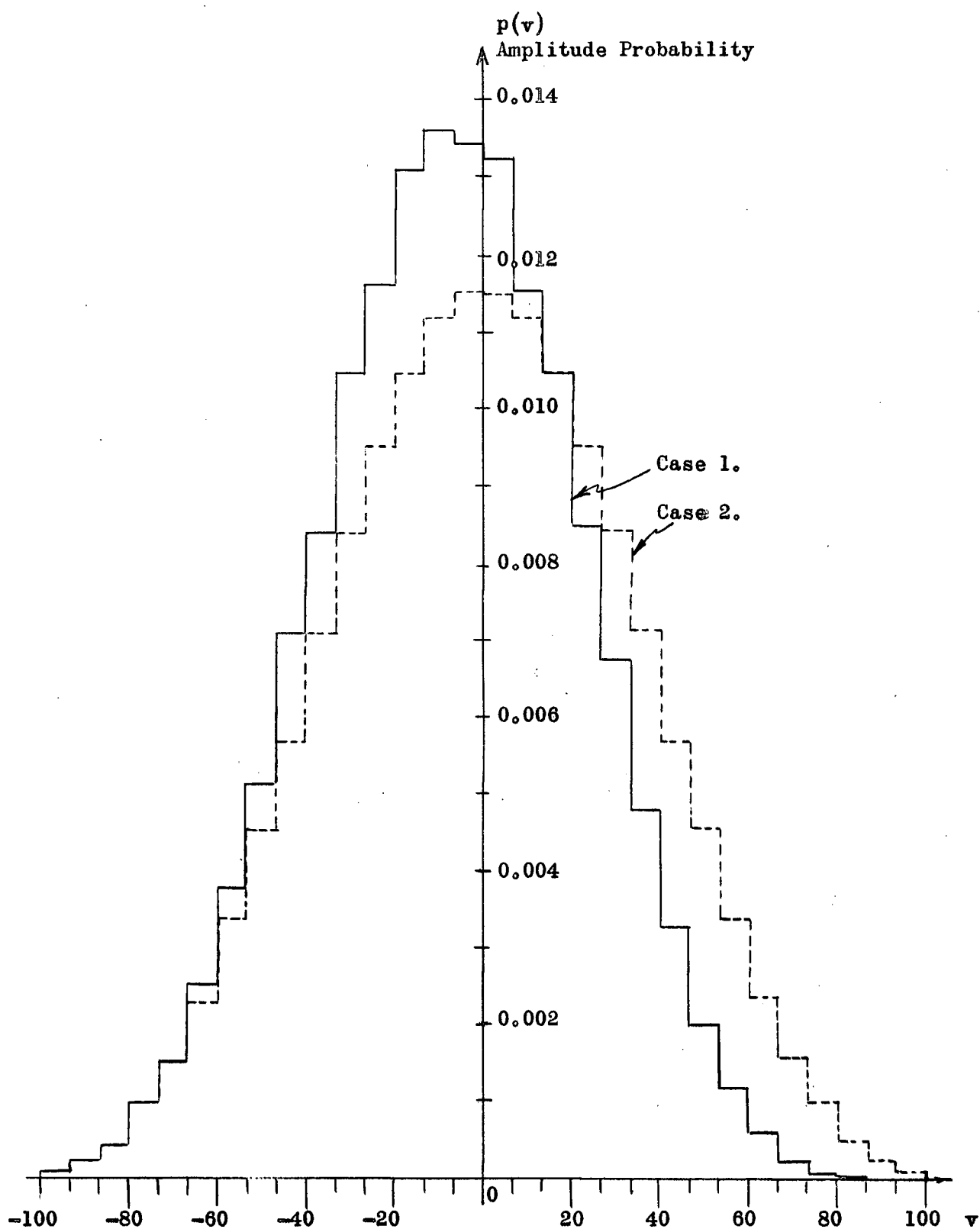


Figure B-1. Theoretical Normalized Amplitude Probability Distributions for two Member Function Sets.

Case 2.

$C_n =$	2	5	9	21	32	48	71	95	119	149	176
$n =$	0	1	2	3	4	5	6	7	8	9	10
$C_n =$	200	220	235	242	241	235	221	200	177	150	119
$n =$	11	12	13	14	15	16	17	18	19	20	21
$C_n =$	96	71	49	33	21	10	5	2	1		
$n =$	22	23	24	25	26	27	28	29	30		

Appendix C.

C-1. Programme for Determining the Cardinal Points of the Theoretical Autocorrelation Functions.

Because of the simple straight-line relationship between $\phi(n\tau_i)$ and $\phi((n+1)\tau_i)$ of the member function autocorrelation functions, it was sufficient to determine the values of the cardinal points $\phi(n\tau_i)$, $n = 0, 1, \dots, \frac{N}{2}$, where the period of the function is equal to $N\tau_i$. The value of $\phi(n\tau_i)$ is given by the formula:

$$\phi(n\tau_i) = \frac{1}{N} (V(0\tau_i)V(n\tau_i) + V(1\tau_i)V((n+1)\tau_i) + \dots \\ + V((N-1)\tau_i)V((N-1+n)\tau_i)) .$$

The equivalent computer problem is: Given N integers, a_1, a_2, \dots, a_N , compute the values of: $(a_1)^2 + (a_2)^2 + \dots + (a_N)^2 = \phi(0)$,

$$\begin{aligned} a_1a_2 + a_2a_3 + \dots + a_Na_1 &= \phi(1\tau_i) \\ a_1a_3 + a_2a_4 + \dots + a_Na_2 &= \phi(2\tau_i) \\ \vdots &\vdots \\ a_1a_{\frac{N}{2}} + a_2a_{\frac{N}{2}+1} + \dots + a_Na_{\frac{N}{2}} &= \phi\left(\frac{N}{2}\tau_i\right) \end{aligned}$$

where a_1 corresponds to $V(0\tau_i)$

a_2 corresponds to $V(1\tau_i)$ etc.

A programme was written which did exactly this. A copy of the programme tape is given on the following page.

```

a004
871e5b43 11604800 67514dd1 001000c4
11604d47 17dc5747 794ef701 00000000
615f4d49 78004820 871f7953 000000c1
4d51a110 17495747 5b5e1160 00010000
4dc14dd1 4000e600 28004953 00000000
4147bd4f bd53c553 175a1b40 00000002
ef57c55b 1751575b c35b11cd 00000000
57475b4b 794fa510 05000052 00200000
2822
a0 2e57f0db

```

C-2. Computer Results.

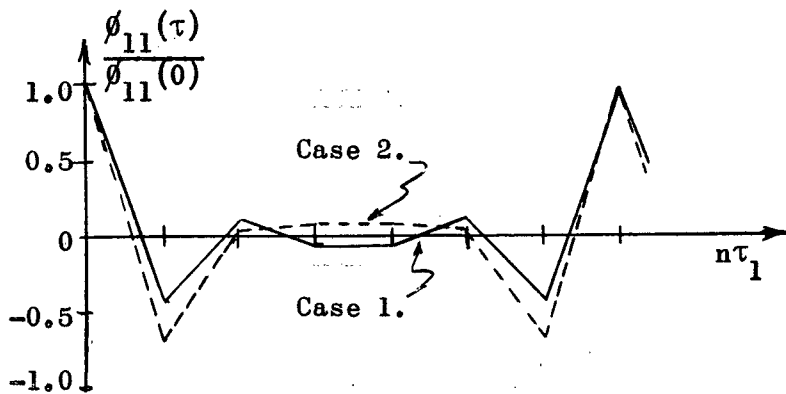
Two determinations of the autocorrelation function were made, corresponding to the two sets of member functions mentioned in Appendix B. Plots of the individual autocorrelation functions for each member function are shown in Figures C-1. (a), (b), and (c). The results of both determinations for the same member function are shown on the same graph.

The computer results for the two determinations are tabulated below. In all cases, the waveform voltage values fed into the computer were made as low as possible by removing common factors. For instance, Case 1., Waveform 1. would be represented as:

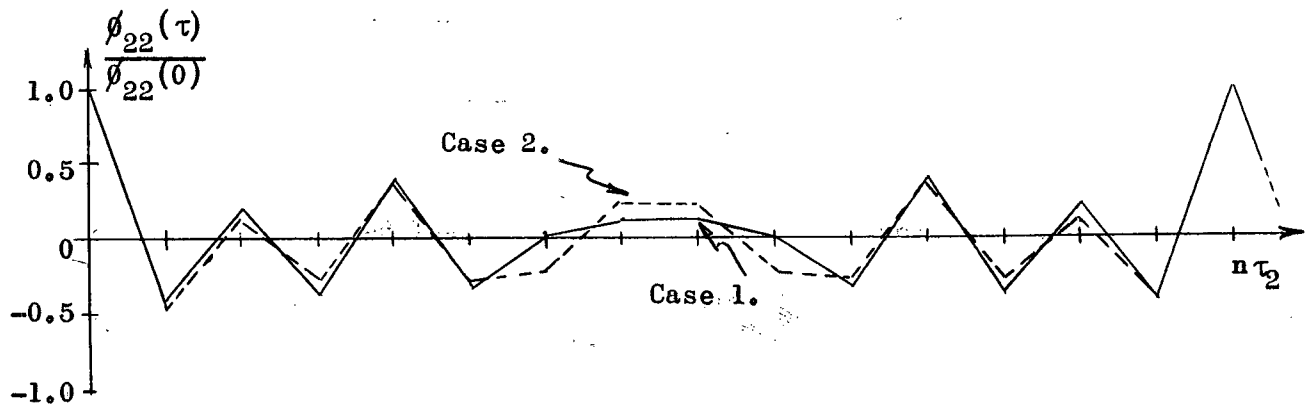
$$V(n \tau_1) = \begin{matrix} -3 & 0 & +1 & -2 & +2 & -1 & 0 \end{matrix}$$

where the factor 280V has been removed. Similarly the common factors 168V and 15V were removed from waveforms 2 and 3 respectively.

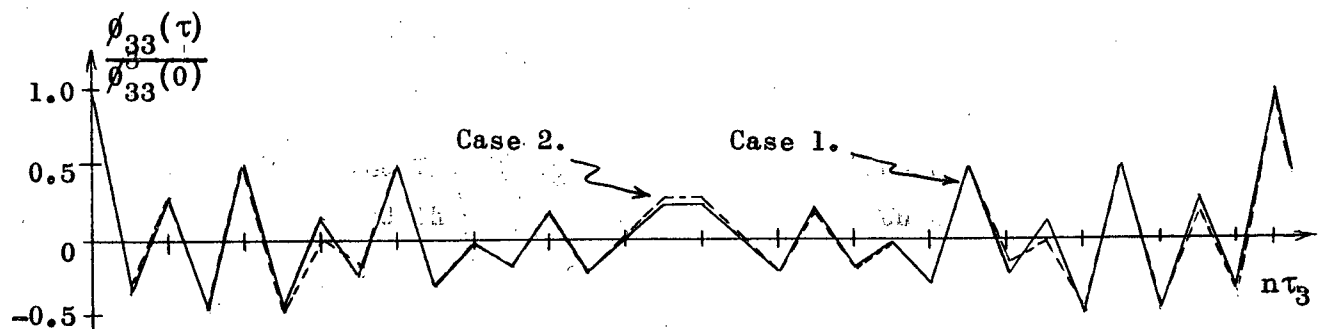
Waveform 1	n =	0	1	2	3
Case 1.	$\phi(n \tau_1) =$	19	-8	4	-1
Case 2.	$\phi(n \tau_1) =$	28	-17	1	2



a) Normalized Theoretical Autocorrelation Functions for Waveform One, Case 1 and Case 2.



b) Normalized Theoretical Autocorrelation Functions for Waveform Two, Case 1 and Case 2.



c) Normalized Theoretical Autocorrelation Functions for Waveform Three, Case 1 and Case 2.

Figure C-1. Theoretical Normalized Autocorrelation Functions.

Waveform 2. $n =$ 0 1 2 3 4 5 6 7

Case 1. $\phi(n\tau_2) =$ 95 -38 19 -34 38 -31 00 11

Case 2. $\phi(n\tau_2) =$ 120 -53 14 -31 43 -34 -25 26

Waveform 3. $n =$ 0 1 2 3 4 5

Case 1. $\phi(n\tau_3) =$ 21904 -7813 6246 -9967 10972 -10497

Case 2. $\phi(n\tau_3) =$ 25040 -9157 6246 -9967 11756 -10833

$n =$ 6 7 8 9 10 11

Case 1. $\phi(n\tau_3) =$ 2762 -5203 10799 -6374 -571 -4240

Case 2. $\phi(n\tau_3) =$ 410 -4195 12143 -9510 -571 -4240

$n =$ 12 13 14 15

Case 1. $\phi(n\tau_3) =$ 4173 -4752 251 4830

Case 2. $\phi(n\tau_3) =$ 4509 -5536 -757 7182

Appendix D

1. Bell, H. Jr. and Rideout, V.C., "A High-Speed Correlator," Transactions of the I.R.E. Professional Group on Electronic Computers, vol. EC-3, no. 2. (June 1954) pp. 30-36.
2. Bennett, R.R. and Fulton, A.S., "The Generation and Measurement of Low Frequency Random Noise," Journal of Applied Physics, vol. 22, no. 2. (September 1951) pp. 1187-1191.
3. Bennett, R.W., "Methods of Solving Noise Problems," Proceedings of I.R.E., vol. 44, no. 5. (May 1956) pp. 609-638.
4. Biernson, G.A., "Fundamental Equations for the Application of Statistical Techniques to Feedback-Control Systems." Transactions of the I.R.E. Professional Group on Automatic Control, vol. AC-2, (February 1957) pp. 56-78.
5. Booton, R.C. Jr., "The Analysis of Nonlinear Control Systems with Random Inputs," Proceedings of Symposium on Nonlinear Circuit Analysis, Ann Arbor, Michigan, Edwards Brothers, Inc., 1953 pp. 369-391.
6. Chance, B., Hughes, V., MacNichol, E.F., Sayre, D. and Williams, F.C., Waveforms, New York, McGraw-Hill, 1949. (Ridenour, L.N., ed., M.I.T. Radiation Laboratory Series. vol. 19.)
7. Diamantides, N.D., "Analogue Computer Generation of Probability Distributions for Operations Research," Transactions of the A.I.E.E., vol. 75, (1956) part I, pp. 86-91.
8. Feller, W., An Introduction to Probability Theory and Its Applications, New York, John Wiley and Sons, Inc., 1950.
9. Fink, H.J., "Precision Frequency Control of a Magnetic Storage Drum," M.A.Sc. Thesis, University of British Columbia, 1956.
10. Forsythe, G.A., "Generation and Testing of Random Digits at the National Bureau of Standards, Los Angeles," Monte Carlo Method, Washington, U.S. Government Printing Office, 1951. (National Bureau of Standards Applied Mathematics Series, vol.12,) pp. 34-35.
11. Hammer, P. C., "The Mid-square Method of Generating Digits," Monte Carlo Method, Washington, U.S. Government Printing Office, 1951. (National Bureau of Standards Applied Mathematics Series, vol. 12,) p. 33.
12. Heaslet, M.A. and Uspensky, J.V., Elementary Number Theory, New York, McGraw-Hill, 1939.

13. James, H.M., Nichols, N.B., and Phillips, R.S., Theory of Servo-Mechanisms, New York, McGraw-Hill, 1947. (Ridenour, L.N., ed., M.I.T. Radiation Laboratory Series, vol. 25.)
14. Johnson, E.C., "Sinusoidal Techniques Applied to Nonlinear Feedback Systems," Proceedings of Symposium on Nonlinear Circuit Analysis, Ann Arbor, Michigan, Edwards Brothers Inc., 1953.
15. Lee Y. W., "Communication Applications of Correlation Analysis," Symposium on Applications of Autocorrelation Analysis to Physical Problems. Washington, Publication of ONR, Department of Navy, 1949. pp. 4-23.
16. Marconi Instruction Folder #131-673, Installing and Operating Instructions, Pulse Amplitude Analyser (Kicksorter) Marconi type 115-935.
17. Millman, J. and Puckett, T.H., "Accurate Linear Bidirectional Gates," Proceedings of I.R.E., vol. 43, no. 1. (January 1955) pp. 29-37.
18. Millman, J. and Taub, H., Pulse and Digital Circuits, New York, McGraw-Hill, 1956.
19. Paynter, H.M., ed., A Palimpsest on the Electronic Analog Art, Boston, Massachusetts, Geo. A. Philbrick Researches, Inc., 1955. p. 197.
20. Philbrick, G.A., Catalog and Manual, Boston, Massachusetts, Geo. A. Philbrick Researches, Inc., 1951.
21. Reintjes, J.F., "An Analogue Electronic Correlator," Proceedings of National Electronics Conference, vol. 7, 1951. pp. 390-400.
22. Truxal, J.G., Control System Synthesis, New York, McGraw-Hill, 1955.
23. van der Ziel, A., Noise, New York, Prentice-Hall, 1954.
24. von Neumann, J., "Various Techniques Used in Connection with Random Digits," Monte Carlo Method, Washington, U.S. Government Printing Office, 1951. (National Bureau of Standards Applied Mathematics Series vol. 12.) pp. 36-38.